Hindawi
International Journal of Aerospace Engineering
Volume 2019, Article ID 4129136, 20 pages
https://doi.org/10.1155/2019/4129136

Research Article

Active Disturbance Rejection Control for Air-Breathing Hypersonic Vehicles Based on Prescribed Performance Function

Chenyang Xu,[1] **Humin Lei**,[1] **and Na Lu**[2]

[1]*Air and Missile Defense College, Air Force Engineering University, Xi'an 710051, China*
[2]*Unit 93142, People's Liberation Army, Chengdu 610044, China*

Correspondence should be addressed to Chenyang Xu; 18729057322@163.com

Received 19 July 2019; Revised 9 October 2019; Accepted 29 October 2019; Published 22 November 2019

Academic Editor: Antonio Concilio

Aiming at the longitudinal motion model of the air-breathing hypersonic vehicles (AHVs) with parameter uncertainties, a new prescribed performance-based active disturbance rejection control (PP-ADRC) method was proposed. First, the AHV model was divided into a velocity subsystem and altitude system. To guarantee the reliability of the control law, the design process was based on the nonaffine form of the AHV model. Unlike the traditional prescribed performance control (PPC), which requires accurate initial tracking errors, by designing a new performance function that does not depend on the initial tracking error and can ensure the small overshoot convergence of the tracking error, the error convergence process can meet the desired dynamic and steady-state performance. Moreover, the designed controller combined with an active disturbance rejection control (ADRC) and extended state observer (ESO) further enhanced the disturbance rejection capability and robustness of the method. To avoid the differential expansion problem and effectively filter out the effects of input noise in the differential signals, a new tracking differentiator was proposed. Finally, the effectiveness of the proposed method was verified by comparative simulations.

1. Introduction

Air-breathing hypersonic vehicles (AHVs) are a new type of aircraft, which fly at speeds greater than Mach 5 at near space altitudes. AHVs exhibit fast flying speeds, strong penetration abilities, and long combat distances. It is difficult to detect and intercept AHVs. AHVs have strong survivability, and they have outstanding advantages in strategy, tactics, and cost-effectiveness compared to traditional aerospace vehicles [1–3]. AHVs have become a priority development direction for all of the aerospace powers competing for air and space rights. However, AHVs are multivariable and strongly coupled nonlinear systems. AHVs have large flight airspaces, and the flight environments are complex and variable, which results in large and fast time-varying characteristics and altitude uncertainty of the AHV model. Thus, the design of the AHV control system involves unprecedented difficulties and challenges [4, 5].

Most of the previous research on the modelling and control of AHVs has mainly focused on the AHV's longitudinal motion plane. On the one hand, the longitudinal motion model is complex enough to require flight control. On the other hand, due to the scramjet engine's extreme sensitivity to the flight attitude, AHVs should avoid horizontal manoeuvres during actual flight [6]. In a previous study [7], a robust L_∞ gain control method was designed for AHVs, which used the Takagi-Sugeno (T-S) fuzzy system to approximate the unknown state of the model. To guarantee the robustness of the control scheme, a new fuzzy disturbance observer was designed to estimate the disturbance. A similar longitudinal elastic model of the AHV was expressed as a T-S fuzzy system [8], and a H_2/H_∞ tracking control law was designed to achieve the robust tracking of the speed and altitude reference inputs. To improve the tracking effect, a nonlinear adaptive back-stepping controller was designed for the AHV based on the back-stepping design [9]. Based on the traditional back-stepping control method, a nonsingular fast terminal sliding model control was applied to control the pitch angle and pitch rate, which optimized the control structure of the back-stepping method and achieved finite time convergence of the system [10]. In one study, an integral sliding model control method was proposed [11]. When there

are model uncertainties and external disturbances, the control scheme can still guarantee finite time convergence of the velocity and altitude tracking errors. Aiming at the attitude control problem of AHVs, a robust fuzzy control method based on a nonlinear switching system was proposed [12], which used a fuzzy system to approximate the unknown function of the model and guaranteed the robustness of the control scheme. Neural control methods for scenarios where the control input of the AHV contained a dead zone [13] and the actuator of the AHV contained failures [14] were studied. Two new neural back-stepping control methods were put forward [15, 16]. The altitude subsystem was rewritten in strict and pure feedback forms. Based on the improved back-stepping strategy, the control scheme was designed, and a minimal learning parameter (MLP) algorithm was applied to reduce the online learning parameters. The tracking simulation results of the velocity and altitude reference input showed that the proposed method exhibited better robustness and control effects. To solve the control problem of a strongly nonlinear model, such as an AHV, in addition to the fuzzy system or neural network used in the above literature to estimate the uncertainty of the model, active disturbance rejection control (ADRC) can also be considered. The ADRC term was first used in [17] where Professor J.Q. Han's unique ideas were first systematically introduced into the English literature. In recent years, many scholars have conducted meaningful work on ADRC. In a previous study [18], ADRC was offered as the basis of a paradigm shift, providing the framework, the objectives, and constraints for future control theory development. For a class of multiple-input multiple-output (MIMO) lower-triangular systems which have uncertain dynamics and disturbance, an ADRC method was designed to solve the control problem [19]. An overview of the concept, principles, and practice of the ADRC was presented in [20]. The key idea of ADRC is to use an extended state observer (ESO) to estimate the total disturbance, which is then compensated in the feedback loop. For a class of nonlinear systems with large uncertainties that come from both internal unknown dynamics and external stochastic disturbance, a novel ESO was designed to estimate both state and total disturbance which included the internal uncertain nonlinear part and the external uncertain stochastic disturbance [21]. To improve the performance of ADRC, a fal-based, single-parameter-tuning ESO was proposed, and the convergence of the fal-based ESO and the output tracking were established [22]. To improve the performance of the tracking differentiator (TD), an ADRC method based on a radial basis function neural network (RBFNN) was proposed [23], which enhanced the robustness and disturbance rejection ability of the method. To assist in the tuning of the parameters of the linear ADRC controller, a tuning rule was proposed to minimize the load disturbance attenuation performance [24]. Based on the existing swarm intelligence algorithms, a parameter tuning optimization design of ADRC was achieved [25]. An in-depth study on the scheme design of an ADRC was conducted and applied to a three-degree-of-freedom pneumatic motion system subject to actuator saturation [26], which achieve good control.

Although the methods in the above literature achieved certain control effects, the research focus was on the robustness and steady-state performance of the AHV closed-loop control system, neglecting the dynamic performance of the control system. However, AHV's super-manoeuvrable, large-envelope, and hypersonic flight demands better dynamic performance of the control system than any other existing aircraft. In most cases, a small control delay will cause significant errors in the hypersonic flight. Therefore, to guarantee the robustness and steady-state accuracy of the control system, more attention should be paid to the dynamic performance and real-time performance of the control system. To consider both the steady-state and dynamic performances, the concept of prescribed performance control was proposed by Charalampos and George [27]. The prescribed performance ensured that the tracking error converged to a prescribed arbitrary small area. Meanwhile, the convergence rate and overshoot met the prescribed conditions. Based on the prescribed performance control, a longitudinal inner-loop controller of the hypersonic vehicle was designed [28]. However, the vehicle was considered to be a pure rigid body and the elastic problem was not considered, which resulted in the limitations of the proposed method. Aiming at the elastic body of the AHV model, a prescribed performance fuzzy back-stepping control method and performance neural back-stepping control method were proposed [29, 30], which guaranteed the steady-state performance and dynamic performance of the control system. However, the above two methods considered the AHV model to be an affine model, which made the reliability of the design method not guaranteed. An AHV adaptive neural control method was designed based on the prescribed performance function, which avoided the cumbersome virtual control law design process [31]. Meanwhile, the accuracy and rapidity of the control system were achieved. However, the proposed method relied too much on the initial value of the tracking error, which resulted in the poor practicality and operability.

In view of the deficiencies of the research in the above studies, an elastic hypersonic vehicle was taken as the research object. In this study, a new prescribed performance function was designed based on the hyperbolic cosine function, which avoided the singular control problem caused by the improper initial value setting. Thus, the steady-state performance and dynamic performance of the control system could be guaranteed. Meanwhile, active disturbance rejection control was introduced and an ESO was designed for each unknown nonaffine function in the AHV system [32], which further guaranteed the control accuracy and the robustness of the method. To address the complexity of the derivative of the virtual control law, a track differentiator was applied to estimate the related signals and signal derivatives. The effectiveness and superiority of the proposed method was verified through the simulation and comparison.

2. AHV Model and Preliminaries

2.1. Model Description. To better describe the longitudinal motion of the AHV, American scholar Parker used the research conclusions of Bolender and Doman [33, 34]

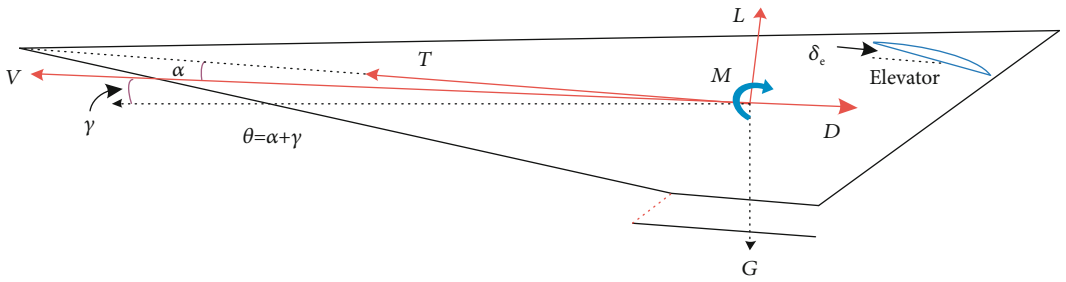

Figure 1: AHV force diagram.

combined with Hooke's law and the Lagrange equation to establish the following control-oriented AHV longitudinal motion parameter fitting model:

$$\dot{V} = \frac{T\cos(\theta-\gamma) - D}{m} - g\sin\gamma, \tag{1}$$

$$\dot{h} = V\sin\gamma, \tag{2}$$

$$\dot{\gamma} = \frac{L + T\sin(\theta-\gamma)}{mV} - \frac{g}{V}\cos\gamma, \tag{3}$$

$$\dot{\theta} = Q, \tag{4}$$

$$\dot{Q} = \frac{M + \tilde{\psi}_1\ddot{\eta}_1 + \tilde{\psi}_2\ddot{\eta}_2}{I_{yy}}, \tag{5}$$

$$k_1\ddot{\eta}_1 = -2\zeta_1\omega_1\dot{\eta}_1 - \omega_1^2\eta_1 + N_1 - \tilde{\psi}_1\frac{M}{I_{yy}} - \frac{\tilde{\psi}_1\tilde{\psi}_2\ddot{\eta}_2}{I_{yy}}, \tag{6}$$

$$k_2\ddot{\eta}_2 = -2\zeta_2\omega_2\dot{\eta}_2 - \omega_2^2\eta_2 + N_2 - \tilde{\psi}_2\frac{M}{I_{yy}} - \frac{\tilde{\psi}_2\tilde{\psi}_1\ddot{\eta}_1}{I_{yy}}. \tag{7}$$

Equations (1)–(5) describe the rigid body part of the AHV. The five rigid states are the velocity V, altitude h, flight-path angle γ, pitch angle θ, and the pitch rate Q. m is the mass of the AHV, g is the gravitational acceleration constant, and I_{yy} is the moment of inertia of the AHV. The force condition of the AHV is shown in Figure 1. The parameter fitting form of the thrust T, drag D, lift L, pitching moment M, and generalized force $N_i(i=1,2)$ can be expressed as follows [35]:

$$\begin{cases} T \approx C_T^{\alpha^3}\alpha^3 + C_T^{\alpha^2}\alpha^2 + C_T^{\alpha}\alpha + C_T^0, \\ D \approx \bar{q}S\left(C_D^{\alpha^2}\alpha^2 + C_D^{\alpha}\alpha + C_D^{\delta_e^2}\delta_e^2 + C_D^{\delta_e}\delta_e + C_D^0\right), \\ L \approx \bar{q}S\left(C_L^{\alpha}\alpha + C_L^{\delta_e}\delta_e + C_L^0\right), \\ M \approx z_T T + \bar{q}S\bar{c}\left[C_{M,\alpha}^{\alpha^2}\alpha^2 + C_{M,\alpha}^{\alpha}\alpha + C_{M,\alpha}^0 + c_e\delta_e\right], \\ N_1 \approx N_1^{\alpha^2}\alpha^2 + N_1^{\alpha}\alpha + N_1^0, \\ N_2 \approx N_2^{\alpha^2}\alpha^2 + N_2^{\alpha}\alpha + N_2^{\delta_e}\delta_e + N_2^0, \end{cases} \tag{8}$$

with

$$\begin{cases} C_T^{\alpha^3} = \beta_1(h,\bar{q})\Phi + \beta_2(h,\bar{q}), \\ C_T^{\alpha^2} = \beta_3(h,\bar{q})\Phi + \beta_4(h,\bar{q}), \\ C_T^{\alpha} = \beta_5(h,\bar{q})\Phi + \beta_6(h,\bar{q}), \\ C_T^0 = \beta_7(h,\bar{q})\Phi + \beta_8(h,\bar{q}), \\ \bar{q} = \dfrac{\bar{\rho}V^2}{2}, \quad \bar{\rho} = \bar{\rho}_0\exp\left(\dfrac{h_0-h}{h_s}\right), \end{cases} \tag{9}$$

where the attack angle $\alpha = \theta - \gamma$, the fuel equivalence ratio Φ, and the elevator angular deflection δ_e are control inputs, S and $\bar{c}$ are the reference area and aerodynamic chord of the AHV, respectively, z_T is the thrust moment arm, c_e is the coefficient of δ_e in M, h_0 and ρ_0 are the nominal altitude and corresponding air density, respectively, $1/h_s$ is the air density decay rate, $\bar{q}$ and $\bar{\rho}$ are dynamic pressure and air density at h, respectively, $C_*^{\bullet^i}(\bullet = \alpha, \delta_e; * = T, D)$ is the ith order coefficient of $\bullet$ in $*$, $C_*^0(* = T, D, L)$ is the constant coefficient in $*$, $C_L^*(* = \alpha, \delta_e)$ is the contribution of the coefficient of $*$ in L, $C_{M,\alpha}^{\alpha^i}$ is the ith order coefficient of α in M, $C_{M,\alpha}^0$ is the constant coefficient in M, $N_j^{\alpha^i}$ is the jth order contribution of α to N_j, N_i^0 is the constant term in N_i, $N_2^{\delta_e}$ is the contribution of δ_e to N_2, and $\beta_i(h,\bar{q})$ is the ith thrust fit parameter.

Equations (6) and (7) describe the elastic body part of the AHV. The elastic states are η_1 and η_2. ζ_i and $\omega_i(i=1,2)$ are the damping ratio and vibrational frequency of the AHV elastic state. k_i and $\tilde{\psi}_i(i=1,2)$ can be expressed as follows:

$$\begin{cases} k_1 = 1 + \dfrac{\tilde{\psi}_1}{I_{yy}}, k_2 = 1 + \dfrac{\tilde{\psi}_2}{I_{yy}}, \\ \tilde{\psi}_1 = \displaystyle\int_{-L_f}^{0} \hat{m}_f\xi\phi_f(\xi)\mathrm{d}\xi, \\ \tilde{\psi}_2 = \displaystyle\int_{0}^{L_a} \hat{m}_a\xi\phi_a(\xi)\mathrm{d}\xi, \end{cases} \tag{10}$$

where L_f and L_a are the front and rear beam length of the AHV, respectively, $\hat{m}_f$ and $\hat{m}_a$ are the mass distributions of the front and the rear beams, respectively, and $\phi_f(\cdot)$ and $\phi_a(\cdot)$ are the vibration mode functions of the front and rear beam, respectively. The specific values of the model

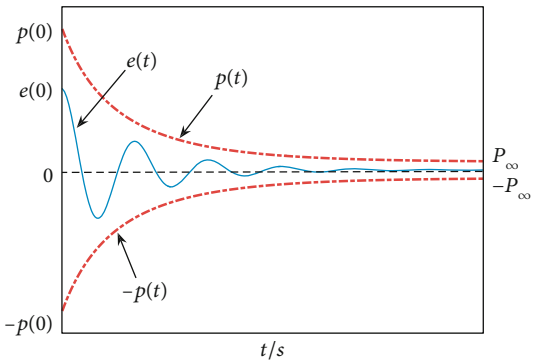

Figure 2: Prescribed performance defined by Equation (12).

parameters and aerodynamic parameters of the abovementioned AHV are shown in [35].

2.2. Prescribed Performance. The AHV prescribed performance control method based on the nonaffine model is studied in this paper. To make the tracking error convergence processes meet the desired dynamic and steady-state performance, the following new performance function $p(t)$ is designed to limit the tracking error.

$$p(t) = \coth\left(k_p t + \chi_p\right) - 1 + p_\infty, \tag{11}$$

where $k_p, \chi_p, p_\infty \in \mathbf{R}^+$ are parameters to be designed.

$p(t)$ has following properties:

(1) $p(t)$ is a positive monotonically decreasing function

(2) $p(0) = \coth(\chi_p) - 1 + p_\infty = e^{2\chi_p} + 1/e^{2\chi_p} - 1 - 1 + p_\infty > p_\infty$

(3) $\lim_{\chi_p \to 0} p(0) \to +\infty$

(4) $\lim_{t \to +\infty} p(t) = p_\infty$

The prescribed performance is defined as follows:

$$-p(t) < e(t) < p(t), \tag{12}$$

where $e(t)$ is the tracking error. By choosing a small enough χ_p, it is guaranteed that $p(t) \to +\infty$ and $-p(t) \to -\infty$ based on the property (3). Therefore, for any unknown but bounded $e(0)$, the following inequality always holds:

$$-p(0) < e(0) < p(0). \tag{13}$$

The prescribed performance defined by Equation (12) is shown in Figure 2. p_∞ is the upper bound of the $e(t)$ steady-state value, which means $-p_\infty < e(\infty) < p_\infty$. Therefore, the desired steady-state accuracy of $e(t)$ can be guaranteed by choosing an appropriate p_∞. $p(0)$ is the maximum overshoot allowed by $e(t)$. k_p directly influences the decreasing rate of $p(t)$. With the increase in k_p, $p(t)$ decreases more rapidly.

Remark 1. For any arbitrary bounded $e(0)$ whether it is known or not, as long as the χ_p is chosen to be small enough, $e(0)$ must be included in the prescribed area defined by Equation (12), which avoids the singular control problem caused by the improper initial value setting of the traditional performance function [36].

Remark 2. When the χ_p is chosen to be small, the value of $p(0)$ will be very large, which can lead to too large of an overshoot of $e(t)$. However, because the response speed of $e(t)$ is limited, the desired dynamic performance, including the overshoot and setting time, can be guaranteed by choosing a larger k_p. This suggests that if the tracking error $e(t)$ satisfies Equation (12), the overshoot and the adjusting time can be constrained within a certain range, as shown in Figure 2. Thus, by designing the controller which can make the tracking error meet the constraint of Equation (12), the desired dynamic performance of the control system can be guaranteed.

The transformed error $\varepsilon(t)$ is defined as follows:

$$\varepsilon(t) = \ln\left(\frac{\lambda(t) + 1}{1 - \lambda(t)}\right), \tag{14}$$

where $\lambda(t) = e(t)/p(t)$. The following theorem can be obtained.

Theorem 1. *If $\varepsilon(t)$ is bounded, then $-p(t) < e(t) < p(t)$.*

Proof. Because $\varepsilon(t)$ is bounded, there must be a bounded constant $\varepsilon_M \in \mathbf{R}^+$ that makes $|\varepsilon(t)| \le \varepsilon_M$. Furthermore, the inverse transformation of Equation (14) is as follows:

$$e^{\varepsilon(t)} = \frac{\lambda(t) + 1}{1 - \lambda(t)}. \tag{15}$$

Based on Equation (15),

$$-1 < \frac{e^{-\varepsilon_M} - 1}{1 + e^{-\varepsilon_M}} \le \lambda(t) \le \frac{e^{\varepsilon_M} - 1}{1 + e^{\varepsilon_M}} < 1. \tag{16}$$

Substituting $\lambda(t) = e(t)/p(t)$ into Equation (16) yields

$$-p(t) < e(t) < p(t). \tag{17}$$

Therefore, Theorem 1 is established.

Remark 3. The control law below will be designed based on the transformed error $\varepsilon(t)$. Theorem 1 shows that as long as $\varepsilon(t)$ is bounded, $e(t)$ can be limited to the prescribed area defined by Equation (12). By choosing appropriate design parameters for $p(t)$, the desired dynamic performance and steady-state accuracy of $e(t)$ can be guaranteed.

2.3. Model Conversion and Control Objective. On the one hand, since the thrust T is directly influenced by the fuel equivalence ratio Φ, the velocity V of the AHV is mainly

controlled by Φ. On the other hand, since the elevator angular deflection δ_e directly influences the pitch rate Q, it further changes the pitch rate θ and the flight-path angle and finally influences the change of the altitude. The altitude change of the AHV is mainly controlled by the elevator angular deflection δ_e [37, 38]. Therefore, most previous studies on AHV control issues first divide the AHV model into a velocity subsystem controlled by Φ (Equation (1)) and an altitude subsystem controlled by δ_e (Equations (2)–(5)) and then derived control laws [39, 40].

Based on the previous studies [37, 38], the velocity subsystem of the AHV was considered to be a nonaffine form with the control input:

$$\begin{cases} \dot{V} = f_V(V, \Phi), \\ y_V = V, \end{cases} \tag{18}$$

where y_V is the output of the system, and $f_V(V, \Phi)$ is a completely unknown continuous differentiable function. For the velocity subsystem, the control goal is to design an appropriate control law Φ based on the nonaffine model (Equation (18)). Thus, the robustness tracking of the velocity V to the reference input V_{ref} can be achieved, and the velocity tracking error can be limited to the prescribed area.

Similarly, the altitude subsystem of the AHV can be expressed as the following nonaffine pure feedback system:

$$\begin{cases} \dot{h} = V \sin \gamma, \\ \dot{\gamma} = f_\gamma(\gamma, \theta), \\ \dot{\theta} = Q, \\ \dot{Q} = f_Q(x, \delta_e), \\ y_h = h, \end{cases} \tag{19}$$

where y_h is the output of the system, and $x = [\gamma, \theta, Q]^T$, $f_\gamma(\gamma, \theta)$, and $f_Q(x, \delta_e)$ are completely unknown continuous differentiable function. For the altitude subsystem, the control goal is to design an appropriate control law δ_e. Thus, the stable tracking of the altitude h to the reference input h_{ref} can be achieved and the altitude tracking error can be limited to the prescribed area. Also, the desired dynamic performance and steady-state accuracy can be guaranteed.

Remark 4. Most previous studies on AHV control issues designed the control law based on the affine model. However, the AHV motion model is nonaffine. If the nonaffine model of the AHV is forcibly simplified to an affine model, the loss of certain key dynamics is inevitably. The designed control law has the risk of partial or complete failure. The proposed control law in this paper will be designed based on the nonaffine model (Equations (18) and (19)), which guarantees the reliability of the control law.

2.4. Extend States Observer and Tracking Differentiator. To design the active disturbance rejection control law, the extended state observer is applied to estimate the uncertainty of the AHV model and the external disturbance. The following system is considered:

$$\dot{z} = H(t) + BU, \tag{20}$$

where $H(t)$ is the unknown term, and U is the input of the subsystem. The state z of the system is measurable. Therefore, the state of the system can be expanded to the following system:

$$\begin{cases} \dot{z} = z_0 + BU, \\ \dot{z}_0 = G(t), \end{cases} \tag{21}$$

where $G(t)$ is the unknown derivative of the unknown term $H(t)$. Therefore, the ESO can be established as follows:

$$\begin{cases} E = Z_1 - z, \\ \dot{Z}_1 = Z_2 - \beta_{01} f_{c1}(E) + BU, \\ \dot{Z}_2 = -\beta_{02} f_{c2}(E), \end{cases} \tag{22}$$

where E is the estimation error of the ESO, Z_1 and Z_2 are the outputs of the ESO, $\beta_{01} > 0$ and $\beta_{02} > 0$ are the observer gains, and parametric function $f_{ci}(\cdot)(i = 1, 2)$ is an appropriately constructed nonlinear function, which satisfies $ef_{ci}(e) > 0$, $\forall e \neq 0$, and $f_{ci}(0) = 0$. The parametric function $f_{ci}(\cdot)$ in this paper is chosen to have the following form:

$$\begin{cases} f_{c1}(E) = E, \\ f_{c2}(E) = |E|^{\alpha_1} \operatorname{sgn}(E), \end{cases} \tag{23}$$

where $0 \leq \alpha_1 \leq 1$.

Theorem 2. *Aiming at the system specified by Equation (20), if the ESO (Equation (22)) is applied, there will be gain parameters $\beta_{01}, \beta_{02} > 0$ and $0 \leq \alpha_1 \leq 1$, which makes the output of the ESO Z_1 and Z_2 converge to the actual state z and a compact set of the unknown term $H(t)$, respectively. Bounded constants $\sigma_1, \sigma_2 > 0$ exist, which make:*

$$\begin{cases} |Z_1 - z| \leq \sigma_1, \\ |Z_2 - H(t)| \leq \sigma_2. \end{cases} \tag{24}$$

Proof. The proof process is shown in the appendix.

Some signals in the control law design process are often difficult to obtain by the model construction. Many scholars have proposed using the tracking differentiator to estimate the signal [41]. The design principle is to achieve the highest precision extraction of the differential signal and to ensure certain robustness to the input noise of the signal. A new TD is proposed in this paper to estimate the differential signal. The specific form of the new TD is as follows:

$$\begin{cases} \dot{v}_1 = v_2, \\ \dot{v}_2 = v_3, \\ \quad \vdots \\ \dot{v}_n = R^n \left(v - v_1 - \dfrac{v_2}{R} - \dfrac{v_3}{R^2} - \cdots - \dfrac{v_n}{R^{n-1}} \right), \end{cases} \tag{25}$$

where v is the input signal to be estimated, v_1 is the estimated value of v, and $v_i (i = 2, 3, \cdots, n)$ are the estimated values of the $i-1$th derivative of v, respectively; R is the parameter to be designed.

Theorem 3. *If the new TD (Equation (25)) is applied to estimate the input signal v and the derivatives, there exists an $R > 0$ that makes $v_i (i = 1, 2, \cdots, n)$ converge to a compact set of $v^{(n)} (n = 0, 1, \cdots, n-1)$, respectively. Bounded constants $\bar{\lambda}_i > 0 (i = 1, 2, \cdots, n)$ exist, which make:*

$$\begin{cases} |v_1 - v| \le \bar{\lambda}_1, \\ |v_2 - \dot{v}| \le \bar{\lambda}_2, \\ \quad \vdots \\ \left| v_n - v^{(n-1)} \right| \le \bar{\lambda}_n. \end{cases} \tag{26}$$

Proof. The certification process is detailed elsewhere [42].

Remark 5. Compared with traditional tracking differentiators [41], the new TD proposed in this paper has two advantages. First, the structure is simple and can estimate the arbitrary derivative of the input signal. Second, the new TD has only one parameter R to be designed, and the parameter adjustment process is easier.

3. Controller Design

3.1. Velocity Controller Design. The velocity subsystem (Equation (18)) is assumed to be affected by external disturbances. According to the idea of self-interference, it can be expressed as follows:

$$\begin{cases} \dot{V} = f_V(V, \Phi) + d_V(t) - l_V \Phi + l_V \Phi \\ \quad = F_V(V, \Phi) + l_V \Phi, \\ y_V = V, \end{cases} \tag{27}$$

where $d_V(t)$ is the external disturbance, $F_V(V, \Phi) = f_V(V, \Phi) + d_V(t) - l_V \Phi$ is the unknown term, and $l_V > 0$ is the parameter to be designed.

The velocity tracking error can be defined as follows:

$$\tilde{V} = V - V_{\text{ref}}. \tag{28}$$

The first derivative of Equation (28) with respect to time is obtained, and Equation (27) is substituted into the result, yielding the following:

$$\dot{\tilde{V}} = F_V(V, \Phi) - \dot{V}_{\text{ref}} + l_V \Phi. \tag{29}$$

According to Equation (14), the velocity transformed error can be defined as follows:

$$\varepsilon_V(t) = \ln \left(\frac{\tilde{V}/p_V(t) + 1}{1 - \tilde{V}/p_V(t)} \right), \tag{30}$$

where $p_V(t) = \coth (k_{pV} t + \chi_{pV}) - 1 + p_{V\infty}$, and $k_{pV}, \chi_{pV}, p_{V\infty} \in \mathbf{R}^+$ are parameters to be designed.

The first derivative of Equation (30) with respect to time is obtained, and Equation (29) is substituted into the result, yielding the following:

$$\begin{aligned} \dot{\varepsilon}_V(t) &= r_V \left(\dot{\tilde{V}} - \frac{\dot{p}_V(t)}{p_V(t)} \tilde{V} \right) \\ &= r_V \left(F_V(V, \Phi) - \dot{V}_{\text{ref}} + l_V \Phi - \frac{\dot{p}_V(t)}{p_V(t)} \tilde{V} \right), \end{aligned} \tag{31}$$

where

$$\begin{aligned} r_V &= \frac{1}{p_V(t)} \left(\frac{1}{\tilde{V}/p_V(t) + 1} - \frac{1}{\tilde{V}/p_V(t) - 1} \right) > 0, \\ \dot{p}_V(t) &= k_{pV} \left(1 - \coth^2 \left(k_{pV} t + \chi_{pV} \right) \right). \end{aligned} \tag{32}$$

To estimate the unknown term $F_V(V, \Phi)$, the following ESO is designed for Equation (31):

$$\begin{cases} E_V = Z_{V1} - \varepsilon_V, \\ \dot{Z}_{V1} = Z_{V2} - \beta_{V1} E_V + r_V \left(l_V \Phi - \dot{V}_{\text{ref}} - \dfrac{\dot{p}_V(t)}{p_V(t)} \tilde{V} \right), \\ \dot{Z}_{V2} = -\beta_{V2} |E_V|^{\alpha_V} \operatorname{sgn}(E_V), \end{cases} \tag{33}$$

where $\beta_{V1}, \beta_{V2} > 0$, $0 \le \alpha_V \le 1$ is the parameter to be designed, Z_{V1} is the estimated value of ε_V, and Z_{V2}/r_V is the estimated value of the unknown term $F_V(V, \Phi)$.

The active disturbance rejection control law Φ can be designed as follows:

$$\Phi = -\frac{1}{l_V} \left(\frac{Z_{V2}}{r_V} + k_V \varepsilon_V - \dot{V}_{\text{ref}} - \frac{\dot{p}_V(t)}{p_V(t)} \tilde{V} \right), \tag{34}$$

where $k_V > 0$ is the parameter to be designed.

Theorem 4. *Considering the velocity subsystem (Equation (18)), if the active disturbance rejection control law (Equation (33)) and the ESO (Equation (32)) are applied, the closed-loop control system is semiglobally uniformly asymptotically stable, and the speed tracking error is limited to the prescribed area. The following inequality holds $-p_V(t) < \tilde{V} < p_V(t)$.*

Proof. Substituting Equation (33) into Equation (31) yields:

$$\dot{\varepsilon}_V = r_V\left(F_V(V,\Phi) - \frac{Z_{V2}}{r_V} - k_V\varepsilon_V\right). \tag{35}$$

The following Lyapunov function was selected:

$$W_V = \frac{1}{2}\varepsilon_V^2. \tag{36}$$

The first derivative of W_V with respect to time is obtained, and Equation (34) is substituted into the result, yielding the following:

$$\begin{aligned}\dot{W}_V &= \varepsilon_V r_V\left(F_V(V,\Phi) - \frac{Z_{V2}}{r_V} - k_V\varepsilon_V\right)\\ &= r_V\left(\varepsilon_V\left(F_V(V,\Phi) - \frac{Z_{V2}}{r_V}\right) - k_V\varepsilon_V^2\right).\end{aligned} \tag{37}$$

Combined with Equation (24), a constant ϖ_V exists such that:

$$\left|F_V(V,\Phi) - \frac{Z_{V2}}{r_V}\right| \le \varpi_V. \tag{38}$$

Considering that $r_V > 0$, Equation (37) is substituted into Equation (36), yielding:

$$\begin{aligned}\dot{W}_V &\le r_V\left(-k_V\varepsilon_V^2 + |\varepsilon_V|\varpi_V\right)\\ &\le r_V\left(-\left(k_V - \frac{1}{2}\right)\varepsilon_V^2 + \frac{1}{2}\varpi_V^2\right).\end{aligned} \tag{39}$$

With $k_V > 1/2$, the following compact set is defined:

$$\Omega_{\varepsilon_V} = \left\{\varepsilon_V \,\middle|\, |\varepsilon_V| \le \sqrt{\frac{(1/2)\varpi_V^2}{k_V - 1/2}}\right\}. \tag{40}$$

Combining Equations (38) and (39), if $\varepsilon_V \notin \Omega_{\varepsilon_V}$, then $\dot{W}_V < 0$. Therefore, the closed-loop control system is semi-globally uniformly asymptotically stable, and the velocity transformed error will finally converge to the compact set Ω_{ε_V}. If the estimated accuracy of the ESO is high enough (ϖ_V is small enough) and the k_V is sufficiently large, the radius of the compact Ω_{ε_V} and the ε_V can be sufficiently small.

The above proves that the transformed error is bounded. According to Theorem 1, $-p_V(t) < \tilde{V} < p_V(t)$. The velocity transformed error is limited to the prescribed area.

3.2. Altitude Controller Design. Considering the altitude subsystem (Equation (19)), the altitude tracking error can be defined as $\tilde{h} = h - h_{\text{ref}}$. The altitude transformed error can be defined as follows:

$$\varepsilon_h(t) = \ln\left(\frac{\tilde{h}/p_h(t) + 1}{1 - \tilde{h}/p_h(t)}\right), \tag{41}$$

where $p_h(t) = \coth(k_{ph}t + \chi_{ph}) - 1 + p_{h\infty}$, and $k_{ph}, \chi_{ph}, p_{h\infty} \in \mathbf{R}^+$ are parameters to be designed.

Furthermore, the first derivative of $\varepsilon_h(t)$ with respect to time yields the following:

$$\dot{\varepsilon}_h(t) = r_h\left(\dot{\tilde{h}} - \frac{\dot{p}_h(t)}{p_h(t)}\tilde{h}\right) = r_h\left(V\sin\gamma - \dot{h}_{\text{ref}} - \frac{\dot{p}_h(t)}{p_h(t)}\tilde{h}\right), \tag{42}$$

where

$$\begin{aligned}r_h &= \frac{1}{p_h(t)}\left(\frac{1}{\tilde{h}/p_h(t) + 1} - \frac{1}{\tilde{h}/p_h(t) - 1}\right) > 0,\\ \dot{p}_h(t) &= k_{ph}\left(1 - \coth^2\left(k_{ph}t + \chi_{ph}\right)\right).\end{aligned} \tag{43}$$

The flight-path angle command is defined as follows:

$$\gamma_{\text{d}} = \arcsin\left(\frac{-k_{h1}\varepsilon_h - k_{h2}\int_0^t \varepsilon_h \text{d}\tau + \dot{h}_{\text{ref}} + \dot{p}_h(t)\tilde{h}/p_h(t)}{V}\right), \tag{44}$$

where $k_{h1}, k_{h2} > 0$ are parameters to be designed.

If $\gamma \to \gamma_{\text{d}}$, γ in Equation (41) is replaced with γ_{d} and a Laplace transform is applied, yielding:

$$s^2 + k_{h1}s + k_{h2} = 0. \tag{45}$$

The two characteristics roots of Equation (43), $(-k_{h1} - \sqrt{{k_{h1}}^2 - 4k_{h2}})/2$ and $(-k_{h1} + \sqrt{{k_{h1}}^2 - 4k_{h2}})/2$, are negative real numbers. Therefore, the altitude transformed error $\varepsilon_h(t)$ is convergent and bounded. For the altitude subsystem (Equation (19)), the control goal can be achieved through the control law δ_{e} design which makes $\gamma \to \gamma_{\text{d}}$ [43].

For the rest of the altitude subsystem (Equation (19)), the active disturbance rejection control law of δ_{e} is designed in three steps.

Step 1. For $\dot{\gamma} = f_\gamma(\gamma, \theta)$, the pitch angle command θ_{d} is designed.

Combined with the concept of active disturbance rejection, $\dot{\gamma} = f_\gamma(\gamma, \theta)$ can be expressed as follows:

$$\dot{\gamma} = f_\gamma(\gamma,\theta) + d_\gamma(t) - l_\gamma\theta + l_\gamma\theta = F_\gamma(\gamma,\theta) + l_\gamma\theta, \tag{46}$$

where $d_\gamma(t)$ is the external disturbance, $F_\gamma(\gamma,\theta) = f_\gamma(\gamma,\theta) + d_\gamma(t) - l_\gamma\theta$, and $l_\gamma > 0$ is a parameter to be designed.

The flight-path angle tracking error is defined as follows:

$$\tilde{\gamma} = \gamma - \gamma_{\text{d}}. \tag{47}$$

The first derivative of Equation (45) is obtained, and Equation (44) is substituted into the result, yielding:

$$\dot{\tilde{\gamma}} = \dot{\gamma} - \dot{\gamma}_{\mathrm{d}} = F_{\gamma}(\gamma, \theta) + l_{\gamma}\theta - \dot{\gamma}_{\mathrm{d}}. \tag{48}$$

The mathematical expression of $\dot{\gamma}_{\mathrm{d}}$ is complicated. Thus, to avoid the differential expansion problem and effectively filter out the effects of input noise in the differential signals, the new TD proposed in this paper is applied to estimate $\dot{\gamma}_{\mathrm{d}}$.

$$\begin{cases} \dot{v}_{\gamma 1} = v_{\gamma 2}, \\ \dot{v}_{\gamma 2} = R_{\gamma}^{2}\left(\gamma_{\mathrm{d}} - v_{\gamma 1} - \dfrac{v_{\gamma 2}}{R_{\gamma}}\right), \end{cases} \tag{49}$$

where $R_{\gamma} > 0$ is the parameter to be designed, and $v_{\gamma 1}$ and $v_{\gamma 2}$ are the estimated values of γ_{d} and $\dot{\gamma}_{\mathrm{d}}$, respectively.

To estimate the unknown term $F_{\gamma}(\gamma, \theta)$, the following ESO is designed for Equation (46):

$$\begin{cases} E_{\gamma} = Z_{\gamma 1} - \tilde{\gamma}, \\ \dot{Z}_{\gamma 1} = Z_{\gamma 2} - \beta_{\gamma 1} e_{\gamma} - v_{\gamma 2} + l_{\gamma}\theta, \\ \dot{Z}_{\gamma 2} = -\beta_{\gamma 2}\left|E_{\gamma}\right|^{\alpha_{\gamma}} \operatorname{sgn}\left(E_{\gamma}\right), \end{cases} \tag{50}$$

where $\beta_{\gamma 1}, \beta_{\gamma 2} > 0, 0 \le \alpha_{\gamma} \le 1$ is the parameter to be designed, and $Z_{\gamma 1}$ and $Z_{\gamma 2}$ are the estimated values of $\tilde{\gamma}$ and $F_{\gamma}(\gamma, \theta)$, respectively.

The pitch angle command θ_{d} can be designed as follows:

$$\theta_{\mathrm{d}} = -\frac{1}{l_{\gamma}}\left(Z_{\gamma 2} + k_{\gamma}\tilde{\gamma} - v_{\gamma 2}\right), \tag{51}$$

where $k_{\gamma} > 0$ is the parameter to be designed.

Step 2. For $\dot{\theta} = Q$, the pitch rate command Q_{d} is designed.

The pitch angle tracking error is defined as follows:

$$\tilde{\theta} = \theta - \theta_{\mathrm{d}}. \tag{52}$$

If the AHV is affected by an external disturbance, $\dot{\theta} = Q$ can be expressed as follows:

$$\dot{\theta} = Q + d_{\theta}(t), \tag{53}$$

where $d_{\theta}(t)$ is the unknown external disturbance.

The first derivative of $\tilde{\theta}$ with respect to time is obtained, and Equation (51) is substituted into the result, yielding:

$$\dot{\tilde{\theta}} = \dot{\theta} - \dot{\theta}_{\mathrm{d}} = Q + d_{\theta}(t) - \dot{\theta}_{\mathrm{d}}. \tag{54}$$

To avoid the differential expansion problem and effectively filter out the effects of input noise in the differential signals, the new TD proposed in this paper is applied to estimate $\dot{\theta}_{\mathrm{d}}$:

$$\begin{cases} \dot{v}_{\theta 1} = v_{\theta 2} \\ \dot{v}_{\theta 2} = R_{\theta}^{2}\left(\theta_{\mathrm{d}} - v_{\theta 1} - \dfrac{v_{\theta 2}}{R_{\theta}}\right), \end{cases} \tag{55}$$

where $R_{\theta} > 0$ is the parameter to be designed, and $v_{\theta 1}$ and $v_{\theta 2}$ are the estimated values of θ_{d} and $\dot{\theta}_{\mathrm{d}}$, respectively.

To estimate the unknown term $d_{\theta}(t)$, the following ESO is designed for Equation (52):

$$\begin{cases} E_{\theta} = Z_{\theta 1} - \tilde{\theta}, \\ \dot{Z}_{\theta 1} = Z_{\theta 2} - \beta_{\theta 1} E_{\theta} - v_{\theta 2} + Q, \\ \dot{Z}_{\theta 2} = -\beta_{\theta 2}\left|E_{\theta}\right|^{\alpha_{\theta}} \operatorname{sgn}\left(E_{\theta}\right), \end{cases} \tag{56}$$

where $\beta_{\theta 1}, \beta_{\theta 2} > 0, 0 \le \alpha_{\theta} \le 1$ is the parameter to be designed, $Z_{\theta 1}$ is the estimated value of $\tilde{\theta}$, and $Z_{\theta 2}$ is the estimated value of the unknown term $d_{\theta}(t)$.

The pitch rate command Q_{d} can be designed as follows:

$$Q_{\mathrm{d}} = -\left(Z_{\theta 2} + k_{\theta}\tilde{\theta} + l_{\gamma}\tilde{\gamma} - v_{\theta 2}\right), \tag{57}$$

where $k_{\theta} > 0$ is the parameter to be designed.

Step 3. For $\dot{Q} = f_{Q}(x, \delta_{\mathrm{e}})$, the control law δ_{e} is designed.

The pitch rate tracking error is defined as follows:

$$\tilde{Q} = Q - Q_{\mathrm{d}}. \tag{58}$$

If the AHV is affected by an external disturbance, combined with the concept of active disturbance rejection, the equation $\dot{Q} = f_{Q}(x, \delta_{\mathrm{e}})$ can be expressed as follows:

$$\dot{Q} = f_{Q}(x, \delta_{\mathrm{e}}) + d_{Q}(t) - l_{Q}\delta_{\mathrm{e}} + l_{Q}\delta_{\mathrm{e}} = F_{Q}(x, \delta_{\mathrm{e}}) + l_{Q}\delta_{\mathrm{e}}, \tag{59}$$

where $d_{Q}(t)$ is the external disturbance, $F_{Q}(x, \delta_{\mathrm{e}}) = f_{Q}(x, \delta_{\mathrm{e}}) + d_{Q}(t) - l_{Q}\delta_{\mathrm{e}}$ is the unknown term, and $l_{Q} > 0$ is the parameter to be designed.

The first derivative of $\tilde{Q}$ with respect to time is obtained, and Equation (57) is substituted into the result, yielding:

$$\dot{\tilde{Q}} = \dot{Q} - \dot{Q}_{\mathrm{d}} = F_{Q}(x, \delta_{\mathrm{e}}) + l_{Q}\delta_{\mathrm{e}} - \dot{Q}_{\mathrm{d}}. \tag{60}$$

The following new TD is applied to estimate $\dot{Q}_{\mathrm{d}}$:

$$\begin{cases} \dot{v}_{Q1} = v_{Q2}, \\ \dot{v}_{Q2} = R_{Q}^{2}\left(Q_{\mathrm{d}} - v_{Q1} - \dfrac{v_{Q2}}{R_{Q}}\right), \end{cases} \tag{61}$$

where $R_{Q} > 0$ is the parameter to be designed, and v_{Q1} and v_{Q2} are the estimated values of Q_{d} and $\dot{Q}_{\mathrm{d}}$, respectively.

To estimate the unknown term $F_Q(x, \delta_e)$, the following ESO is designed for Equation (58):

$$\begin{cases} E_Q = Z_{Q1} - \tilde{Q}, \\ \dot{Z}_{Q1} = Z_{Q2} - \beta_{Q1} E_Q - \upsilon_{Q2} + l_Q \delta_e, \\ \dot{Z}_{Q2} = -\beta_{Q2} |E_Q|^{\alpha_Q} \operatorname{sgn}(E_Q), \end{cases} \tag{62}$$

where $\beta_{Q1}, \beta_{Q2} > 0$, $0 \le \alpha_Q \le 1$ is the parameter to be designed, Z_{Q1} is the estimated value of $\tilde{Q}$, and Z_{Q2} is the estimated value of the unknown term $F_Q(x, \delta_e)$.

The control law δ_e can be designed as follows:

$$\delta_e = -\frac{1}{l_Q}\left(Z_{Q2} + k_Q \tilde{Q} - \upsilon_{Q2} + \tilde{\theta}\right), \tag{63}$$

where $l_Q > 0$ is the parameter to be designed.

Theorem 5. *Considering the altitude subsystem (Equation (19)), if the active disturbance rejection control law δ_e (Equation (61)), the ESO (Equation (60)), and the new TD are applied, the closed-loop control system is semiglobally uniformly asymptotically stable. The tracking errors ε_h, $\tilde{\gamma}$, $\tilde{\theta}$, and $\tilde{Q}$ are bounded, and the altitude tracking error $\tilde{h}$ is limited to the prescribed area. The following inequality holds $-p_h(t) < \tilde{h} < p_h(t)$.*

Proof. The following Lyapunov function is selected:

$$W_h = \frac{1}{2}\tilde{\gamma}^2 + \frac{1}{2}\tilde{\theta}^2 + \frac{1}{2}\tilde{Q}^2. \tag{64}$$

The first derivative of W_h with respect to time is obtained, and Equations (46), (49), (50), (52), (55), (56), (58), and (61) are substituted into the result, yielding:

$$\begin{aligned} \dot{W}_h &= \tilde{\gamma}\dot{\tilde{\gamma}} + \tilde{\theta}\dot{\tilde{\theta}} + \tilde{Q}\dot{\tilde{Q}} = \tilde{\gamma}\left(F_\gamma(\gamma,\theta) + l_\gamma\left(\tilde{\theta} + \theta_d\right) - \dot{\gamma}_d\right) \\ &\quad + \tilde{\theta}\left(\tilde{Q} + Q_d + d_\theta(t) - \dot{\theta}_d\right) + \tilde{Q}\left(F_Q(x,\delta_e) + l_Q\delta_e - \dot{Q}_d\right) \\ &= -k_\gamma\tilde{\gamma}^2 + \tilde{\gamma}\left(F_\gamma(\gamma,\theta) - Z_{\gamma 2}\right) + \tilde{\gamma}\left(\upsilon_{\gamma 2} - \dot{\gamma}_d\right) + l_\gamma\tilde{\theta}\tilde{\gamma} \\ &\quad - k_\theta\tilde{\theta}^2 - l_\gamma\tilde{\theta}\tilde{\gamma} + \tilde{\theta}(d_\theta(t) - Z_{\theta 2}) + \tilde{\theta}\left(\upsilon_{\theta 2} - \dot{\theta}_d\right) \\ &\quad + \tilde{\theta}\tilde{Q} - k_Q\tilde{Q}^2 - \tilde{\theta}\tilde{Q} + \tilde{Q}\left(F_Q(x,\delta_e) - Z_{Q2}\right) \\ &\quad + \tilde{Q}\left(\upsilon_{Q2} - \dot{Q}_d\right). \end{aligned} \tag{65}$$

According to Equations (24) and (26), bounded constants σ_γ, σ_θ, σ_Q, $\bar{\lambda}_\gamma$, $\bar{\lambda}_\theta$, and $\bar{\lambda}_Q$ exist, which make:

$$\begin{cases} \left|F_\gamma(\gamma,\theta) - Z_{\gamma 2}\right| \le \sigma_\gamma, \left|\upsilon_{\gamma 2} - \dot{\gamma}_d\right| \le \bar{\lambda}_\gamma, \\ \left|d_\theta(t) - Z_{\theta 2}\right| \le \sigma_\theta, \left|\upsilon_{\theta 2} - \dot{\theta}_d\right| \le \bar{\lambda}_\theta, \\ \left|F_Q(x,\delta_e) - Z_{Q2}\right| \le \sigma_Q, \left|\upsilon_{Q2} - \dot{Q}_d\right| \le \bar{\lambda}_Q, \end{cases} \tag{66}$$

where

$$\begin{cases} \tilde{\gamma}\sigma_\gamma \le \dfrac{\tilde{\gamma}^2}{2} + \dfrac{\sigma_\gamma^2}{2}, \tilde{\gamma}\bar{\lambda}_\gamma \le \dfrac{\tilde{\gamma}^2}{2} + \dfrac{\bar{\lambda}_\gamma^2}{2}, \\ \tilde{\theta}\sigma_\theta \le \dfrac{\tilde{\theta}^2}{2} + \dfrac{\sigma_\theta^2}{2}, \tilde{\theta}\bar{\lambda}_\theta \le \dfrac{\tilde{\theta}^2}{2} + \dfrac{\bar{\lambda}_\theta^2}{2}, \\ \tilde{Q}\sigma_Q \le \dfrac{\tilde{Q}^2}{2} + \dfrac{\sigma_Q^2}{2}, \tilde{Q}\bar{\lambda}_Q \le \dfrac{\tilde{Q}^2}{2} + \dfrac{\bar{\lambda}_Q^2}{2}. \end{cases} \tag{67}$$

Combining Equations (63), (64), and (65) yields the following:

$$\begin{aligned} \dot{W}_h \le &-(k_\gamma - 1)\tilde{\gamma}^2 - (k_\theta - 1)\tilde{\theta}^2 - (k_Q - 1)\tilde{Q}^2 \\ &+ \frac{1}{2}\left(\sigma_\gamma^2 + \bar{\lambda}_\gamma^2 + \sigma_\theta^2 + \bar{\lambda}_\theta^2 + \sigma_Q^2 + \bar{\lambda}_Q^2\right). \end{aligned} \tag{68}$$

With $k_\gamma > 1$, $k_\theta > 1$, and $k_Q > 1$, the following compact sets are defined:

$$\begin{aligned} \Omega_{\tilde{\gamma}} &= \left\{\tilde{\gamma} \middle| |\tilde{\gamma}| \le \sqrt{\frac{\sigma_\gamma^2 + \bar{\lambda}_\gamma^2 + \sigma_\theta^2 + \bar{\lambda}_\theta^2 + \sigma_Q^2 + \bar{\lambda}_Q^2}{2(k_\gamma - 1)}}\right\}, \\ \Omega_{\tilde{\theta}} &= \left\{\tilde{\theta} \middle| |\tilde{\theta}| \le \sqrt{\frac{\sigma_\gamma^2 + \bar{\lambda}_\gamma^2 + \sigma_\theta^2 + \bar{\lambda}_\theta^2 + \sigma_Q^2 + \bar{\lambda}_Q^2}{2(k_\theta - 1)}}\right\}, \\ \Omega_{\tilde{Q}} &= \left\{\tilde{Q} \middle| |\tilde{Q}| \le \sqrt{\frac{\sigma_\gamma^2 + \bar{\lambda}_\gamma^2 + \sigma_\theta^2 + \bar{\lambda}_\theta^2 + \sigma_Q^2 + \bar{\lambda}_Q^2}{2(k_Q - 1)}}\right\}. \end{aligned} \tag{69}$$

According to Equation (67), if $\tilde{\gamma} \notin \Omega_{\tilde{\gamma}}$, $\tilde{\theta} \notin \Omega_{\tilde{\theta}}$, or $\tilde{Q} \notin \Omega_{\tilde{Q}}$, $\dot{W}_h < 0$. W_h decreases until $\tilde{\gamma}$, $\tilde{\theta}$, and $\tilde{Q}$ converge to the compact sets $\Omega_{\tilde{\gamma}}$, $\Omega_{\tilde{\theta}}$, and $\Omega_{\tilde{Q}}$, respectively. Therefore, the closed-loop control system is semiglobally uniformly asymptotically stable. $\tilde{\gamma}$, $\tilde{\theta}$, and $\tilde{Q}$ are ultimately bounded. However, if the estimated error of the ESO and new TD are sufficiently small ($\sigma_\gamma^2 + \bar{\lambda}_\gamma^2 + \sigma_\theta^2 + \bar{\lambda}_\theta^2 + \sigma_Q^2 + \bar{\lambda}_Q^2$ is sufficiently small), the radii of the compact sets $\Omega_{\tilde{\gamma}}$, $\Omega_{\tilde{\theta}}$, and $\Omega_{\tilde{Q}}$ can be sufficiently small, and $\tilde{\gamma}$, $\tilde{\theta}$, and $\tilde{Q}$ can be sufficiently small. If the $\tilde{\gamma}$ is sufficiently small, then $\gamma \to \gamma_d$. According to Equations (40)–(43), the altitude transformed error is bounded. Thus, by Theorem 1, $-p_h(t) < \tilde{h} < p_h(t)$, which means the altitude transformed error is limited to the prescribed area.

4. Simulation Results

Taking the longitudinal motion model of the AHV (Equations (1)–(10)) as the controlled object, the tracking simulations of speed and altitude reference input were carried out. The simulations were solved using the fourth-order Runge-Kutta method, and the simulation step was taken to

be 0.01 s. The initial values of the AHV state variables are shown in Table 1.

The velocity reference command V_{ref} and the altitude reference command h_{ref} are specified by the following second-order system:

$$\frac{V_{\text{ref}}(s)}{V_I(s)} = \frac{h_{\text{ref}}(s)}{h_I(s)} = \frac{\omega_n^2}{s^2 + 2\zeta_n\omega_n s + \omega_n^2}, \tag{70}$$

where the damping ratio $\zeta_n = 0.9$, the natural frequency $\omega_n = 0.1\text{rad/}s$, and V_I and h_I are the input signals of the second-order system.

When the control algorithm proposed in this paper was used for the simulation, the prescribed performance parameters were selected as follows: $k_{pV} = 0.1$, $\chi_{pV} = 0.35$, $p_{V\infty} = 0.08$, $k_{ph} = 0.1$, $\chi_{ph} = 1$, and $p_{h\infty} = 0.01$. The ADRC controller parameters were selected as follows: $l_V = 10$, $k_V = 10$, $k_{h1} = 3.5$, $k_{h2} = 0.1$, $l_\gamma = 2$, $k_\gamma = 50$, $k_\theta = 50$, $l_Q = 10$, and $k_Q = 20$. The designed parameters of the new TD were selected as follows: $R_\gamma = 5$, $R_\theta = 2$, and $R_Q = 2$. The designed parameters of the ESO were selected as follows: $\beta_{V1} = 2$, $\beta_{V2} = 2$, $\alpha_V = 0.4$, $\beta_{\gamma 1} = 2$, $\beta_{\gamma 2} = 2$, $\alpha_\gamma = 0.4$, $\beta_{\theta 1} = 25$, $\beta_{\theta 2} = 25$, $\alpha_\theta = 0.4$, $\beta_{Q1} = 25$, $\beta_{Q2} = 25$, and $\alpha_Q = 0.4$. Simulations were carried out in the following two scenarios.

Scenario 1. The prescribed performance-based active disturbance rejection control (PP-ADRC) method proposed in this paper with the robust back-stepping control method (RBC) from a previous study [44] was compared. The simulation time was set to 100 s. V_I and h_I were selected as a step signal with an amplitude of 200 m/s. To verify the robustness of the proposed method, it was assumed that a 40% perturbation of the aerodynamic parameters existed in the AHV model, which is expressed as $C = C_0[1 + 0.4\sin(0.1\pi t)]$. C_0 represents the nominal value of the aerodynamic parameter and C represents the value of the aerodynamic parameter in the simulation. In addition, an external disturbance was added after 50 s of simulation:

$$d_V = d_\gamma = d_\theta = d_Q = 2\sin(0.1\pi t). \tag{71}$$

The simulation results for Scenario 1 are shown in Figure 3. Figures 3(a)–3(d) show that the velocity and altitude tracking errors were limited to the prescribed area when using the PP-ADRC. Compared with the RBC, the PP-ADRC can guarantee better dynamic performances of the velocity and altitude tracking errors. When there was parameter perturbation and external disturbance, the PP-ADRC exhibited a higher control accuracy and stronger robustness. Figure 3(e) shows that the flight-path angle response of the PP-ADRC was smoother than that of the RBC. Moreover, the PP-ADRC proposed in this paper could estimate the unknown term of the model through the ESO (Figures 3(g) and 3(h)). The virtual reference command and the differential signals could be effectively estimated through the new TD (Figure 3(f)). Thus, the control accuracy of the method is further guaranteed.

Table 1: Initial values of the AHV state variables.

Parameter	Value	Unit
V	2500	m/s
h	27000	m
γ	0	°
θ	1.5	°
Q	0	°/s
η_1	0.29	—
η_2	0.26	—

Scenario 2. The PP-ADRC was compared with the neural back-stepping control method (NBC) from a previous study [45]. The simulation time was set to 300 s. To better reflect the actual manoeuvre of the AHV, V_I was assumed to be a "step" type signal with a step of 150 m/s per 100 s. h_I was assumed to be a square wave signal with a amplitude of 200 m and a period of 200 s. Also, it was assumed that the 40% perturbation of the aerodynamic parameters existed in the AHV model. The following definitions were made:

$$C = \begin{cases} C_0, & 0\text{ s} \le t < 50\text{ s}, \\ C_0[1 + 0.4\sin(0.1\pi t)], & 50\text{ s} \le t < 100\text{ s}, \\ C_0, & 100\text{ s} \le t < 150\text{ s}, \\ C_0[1 + 0.4\sin(0.1\pi t)], & 150\text{ s} \le t < 200\text{ s}, \\ C_0, & 200\text{ s} \le t < 250\text{ s}, \\ C_0[1 + 0.4\sin(0.1\pi t)], & 250\text{ s} \le t \le 300\text{ s}, \end{cases} \tag{72}$$

where C_0 represents the nominal value of the aerodynamic parameter, and C represents the value of the aerodynamic parameter in the simulation. In addition, external disturbances were added after 150 s of simulation: $d_V = d_\gamma = d_\theta = d_Q = 2\sin(0.1\pi t)$.

The simulation results of the Scenario 2 are shown in Figure 4. Figures 4(a)–4(d) show that the dynamic performances and control accuracy of the velocity and altitude tracking errors of the PP-ADRC were better than those of the NBC. Figure 4(e) shows that the flight-path angle response of the PP-ADRC was smoother than that of the NBC. Meanwhile, the PP-ADRC proposed in this paper could estimate the unknown term of the model through the ESO (Figures 4(g) and 4(h)). The virtual reference command and the differential signals could be effectively estimated through the new TD (Figure 4(f)). Thus, the control accuracy of the method was further guaranteed. Figures 4(i)–4(l) show that both of the control methods could achieve the effective suppression of the elastic vibrations.

5. Conclusions

(1) An active disturbance rejection control for an AHV based on the prescribed performance function is

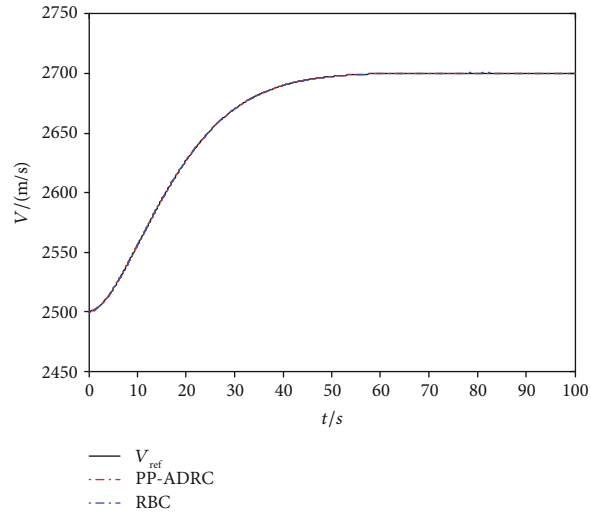

(a) Velocity tracking performance

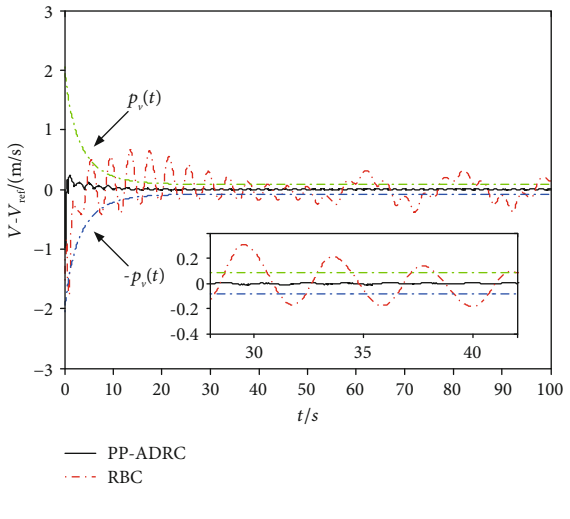

(b) Velocity tracking error

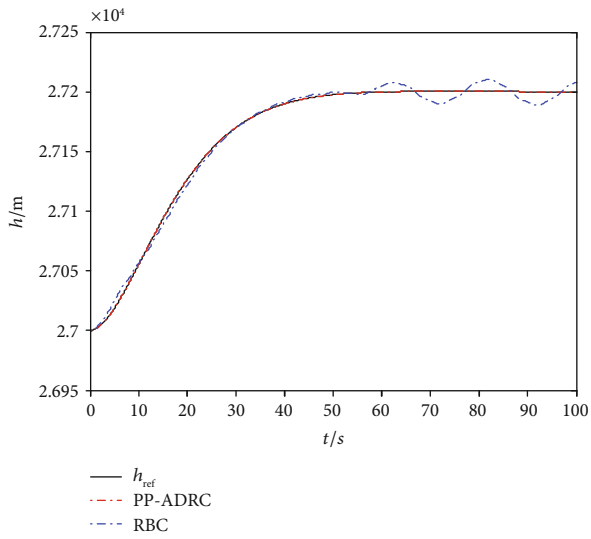

(c) Altitude tracking performance

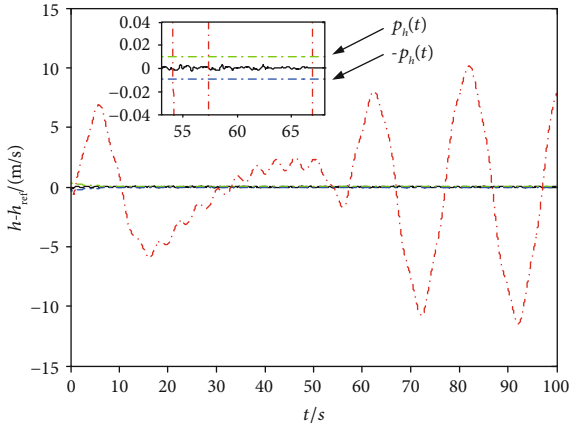

(d) Altitude tracking error

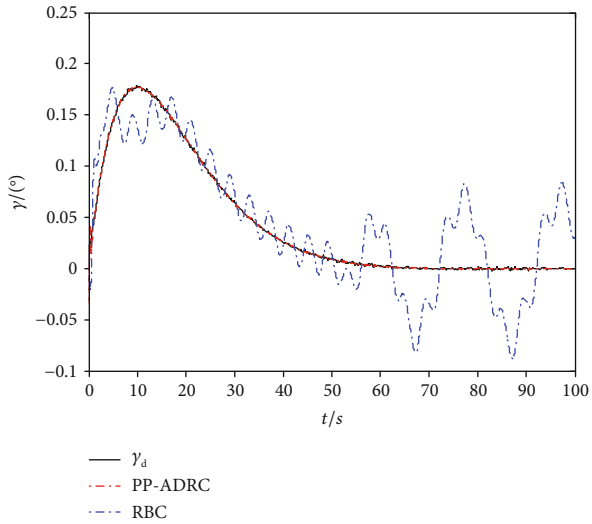

(e) Flight-path angle

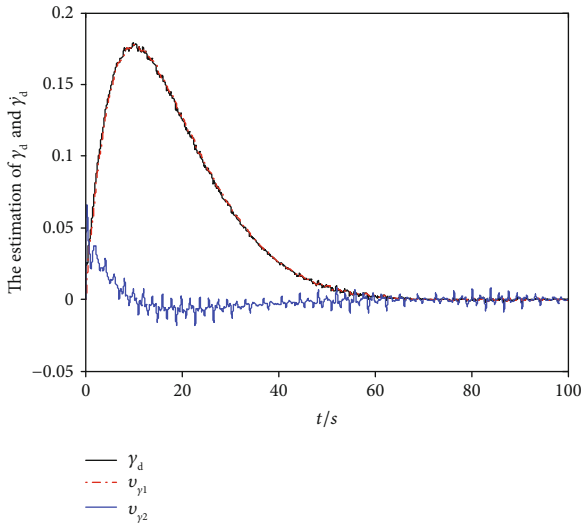

(f) Estimation of γ_d and $\dot{\gamma}_d$

Figure 3: Continued.

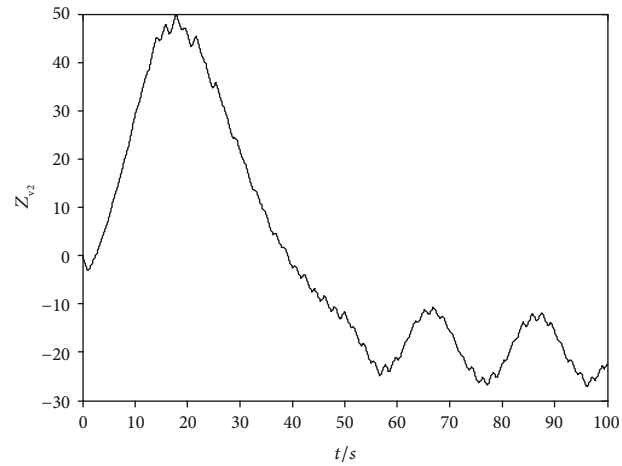

(g) $F_V(V, \Phi)$

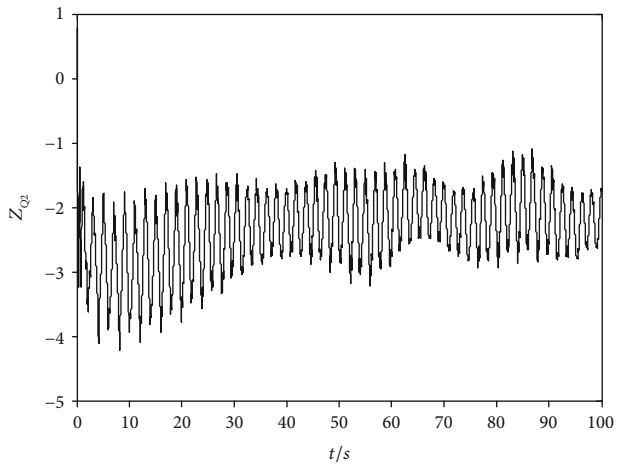

(h) $F_Q(x, \delta_e)$

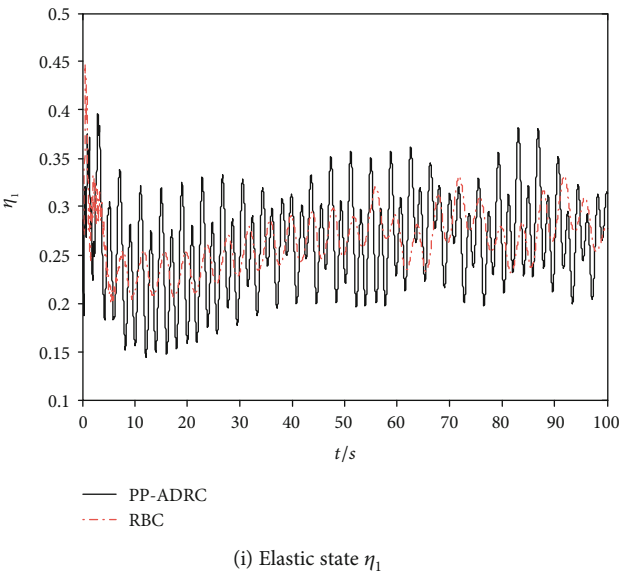

(i) Elastic state η_1

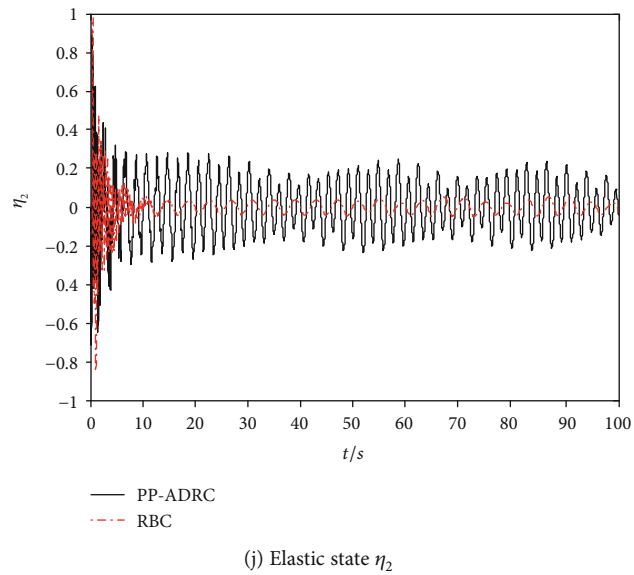

(j) Elastic state η_2

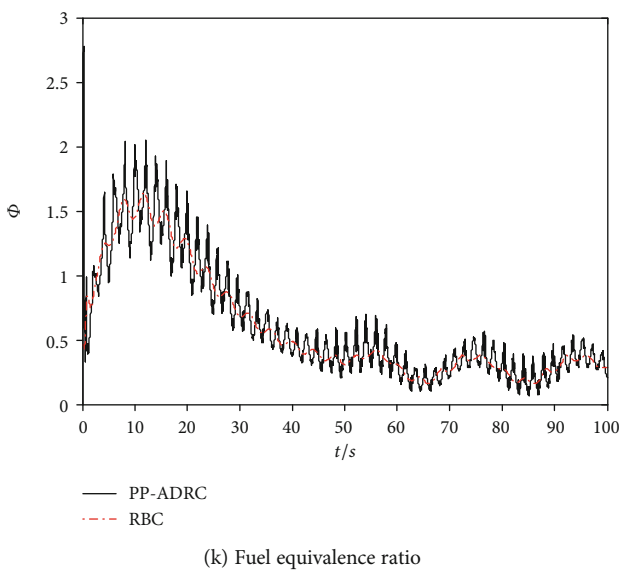

(k) Fuel equivalence ratio

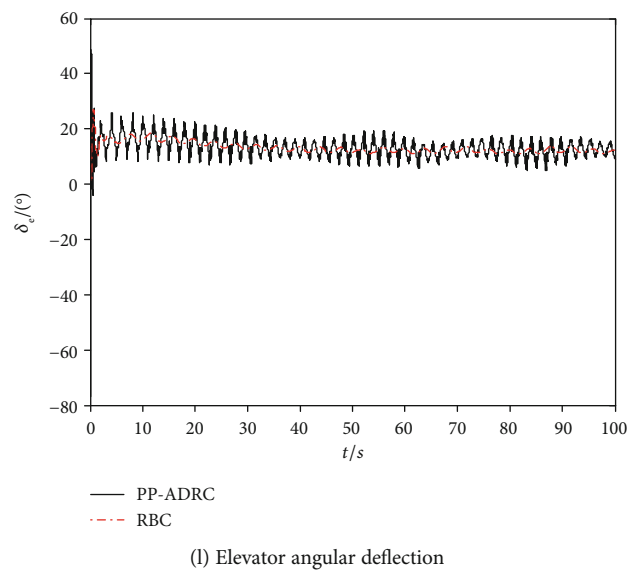

(l) Elevator angular deflection

Figure 3: Simulation results for Scenario 1.

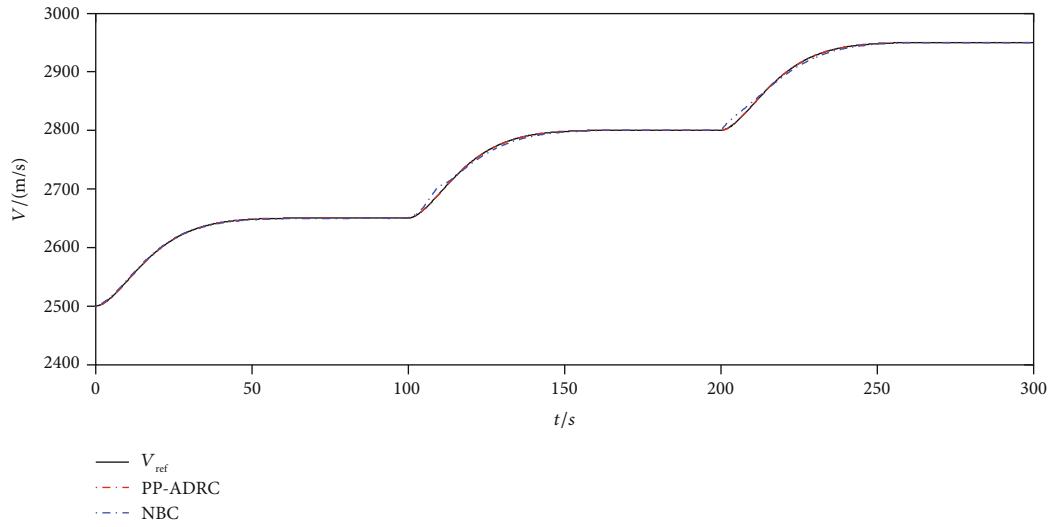

(a) Velocity tracking performance

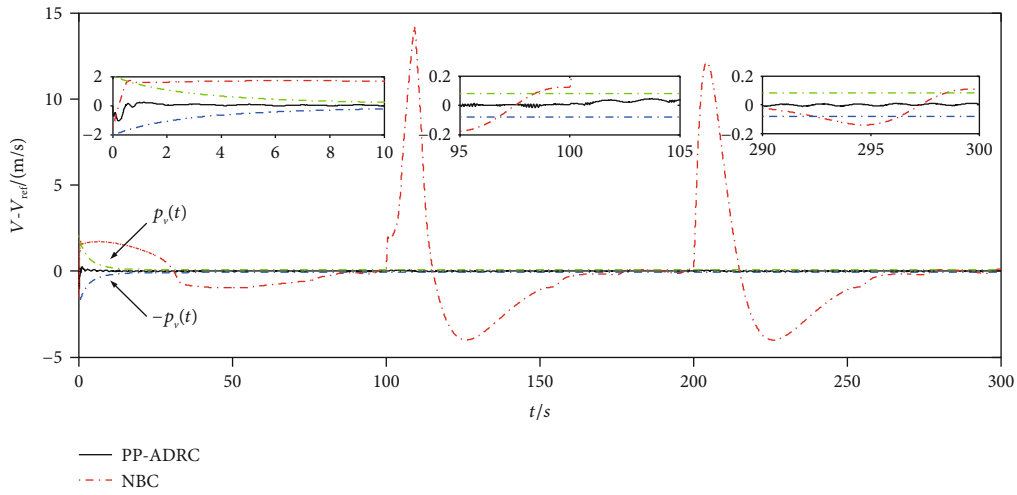

(b) Velocity tracking error

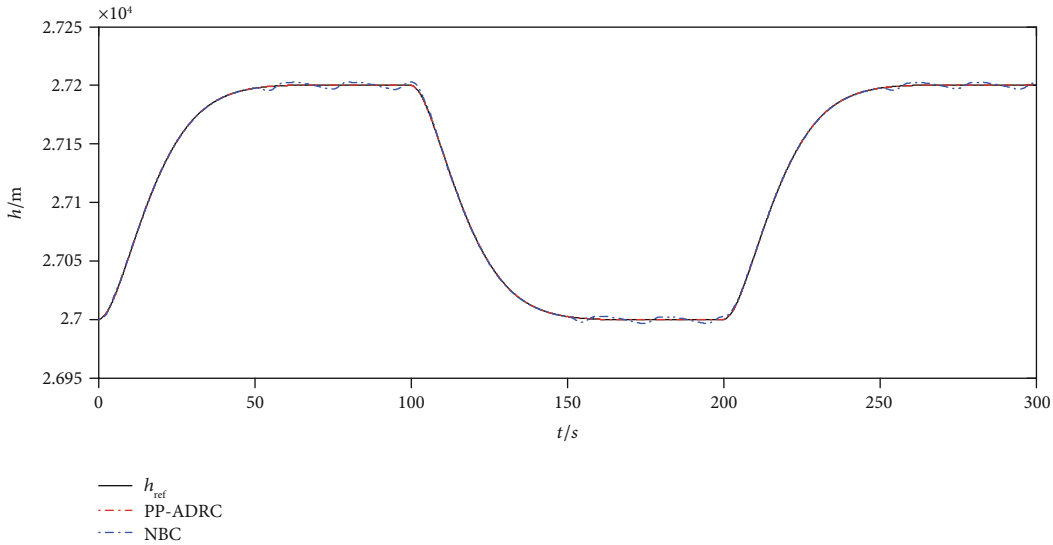

(c) Altitude tracking performance

Figure 4: Continued.

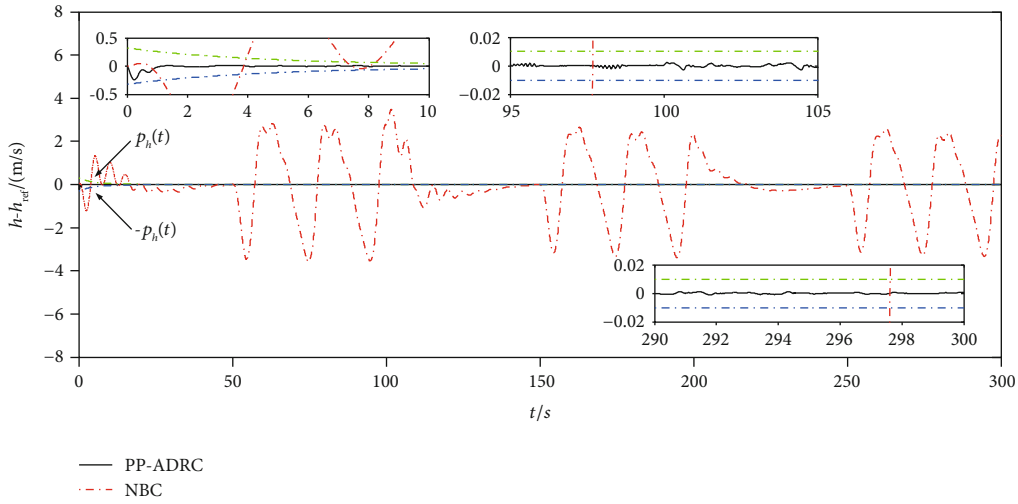

PP-ADRC
NBC

(d) Altitude tracking error

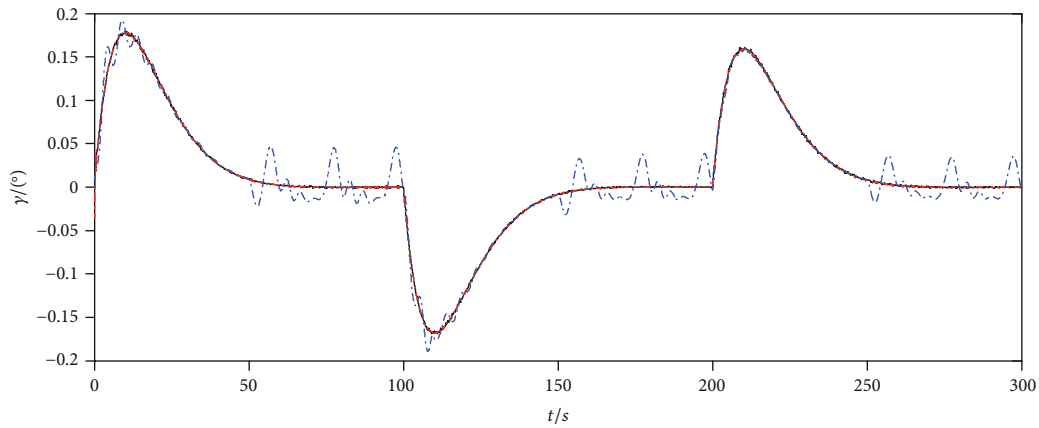

γ_d
PP-ADRC
NBC

(e) Flight-path angle

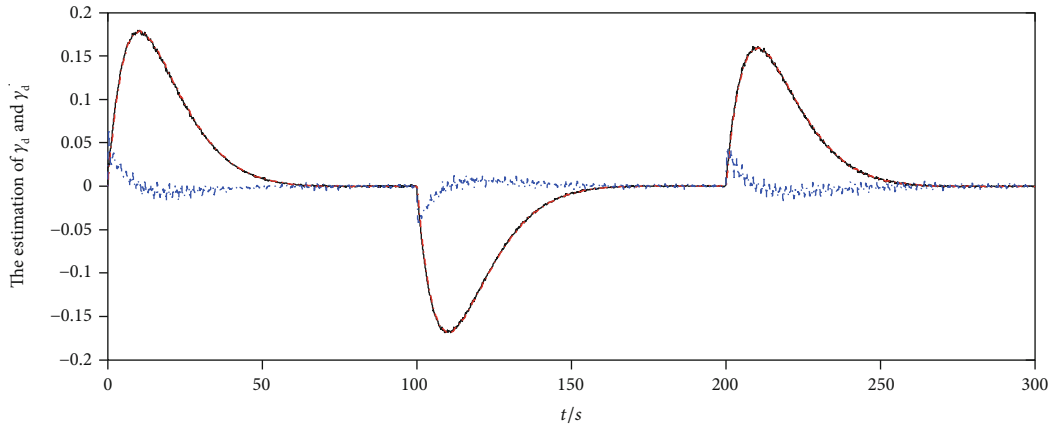

γ_d
$v_{\gamma 1}$
$v_{\gamma 2}$

(f) Estimation of γ_d and $\dot{\gamma}_d$

Figure 4: Continued.

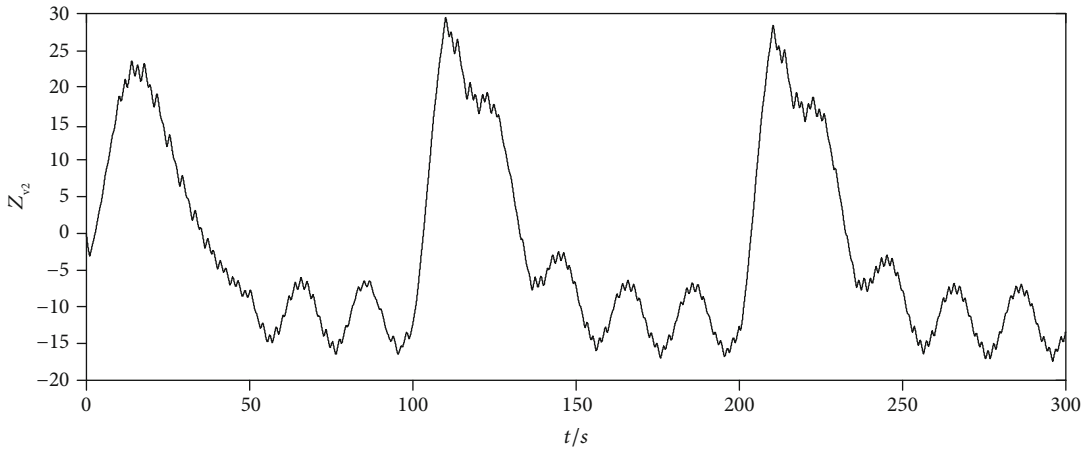

(g) $F_V(V, \Phi)$

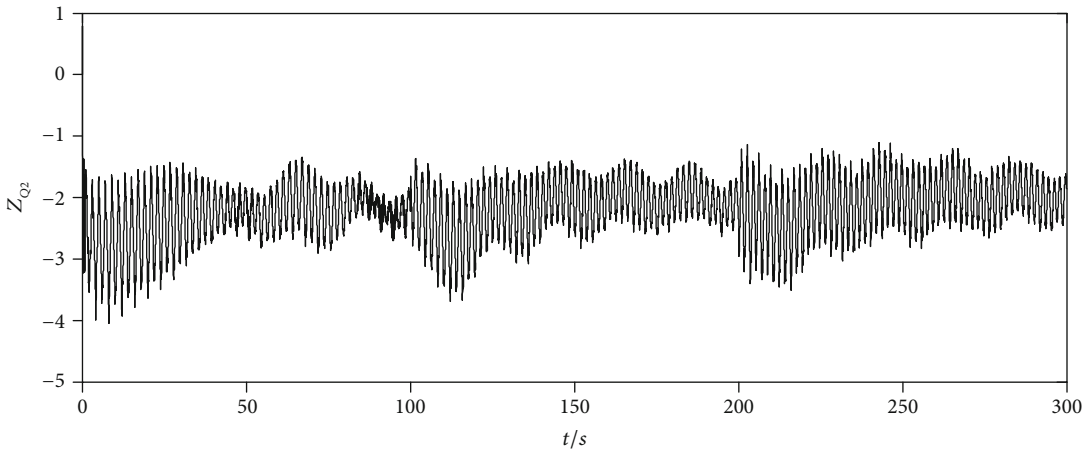

(h) $F_Q(x, \delta_e)$

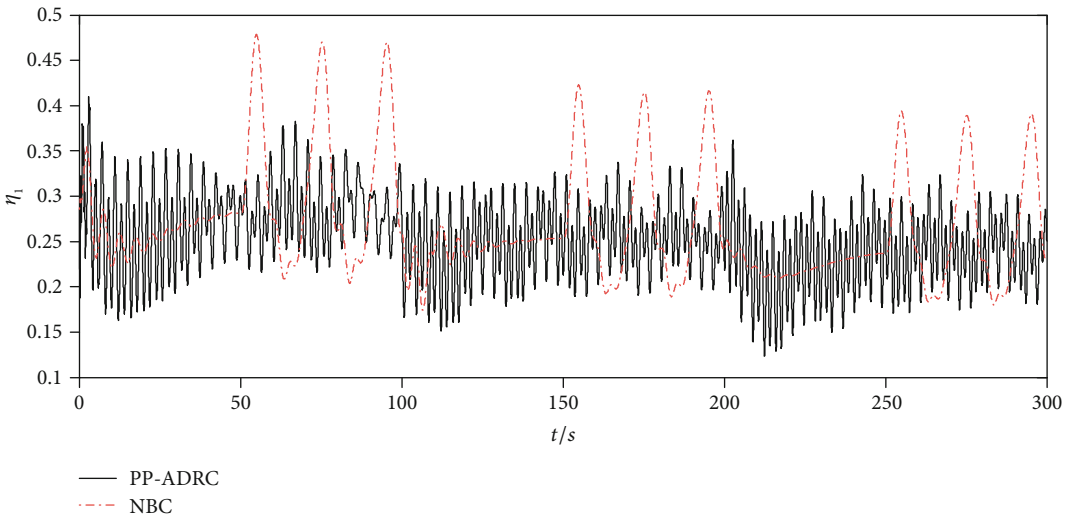

(i) Elastic state η_1

Figure 4: Continued.

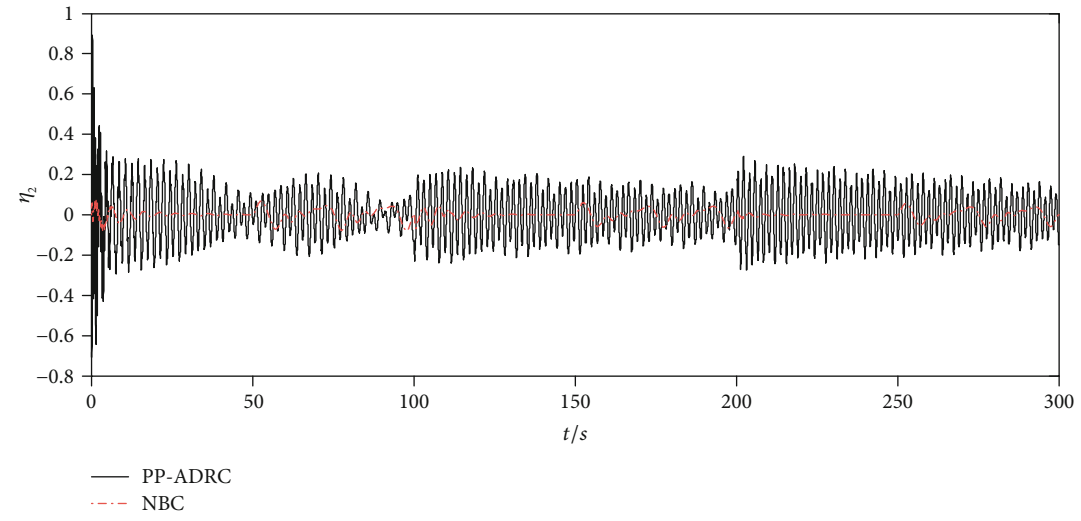

(j) Elastic state η_2

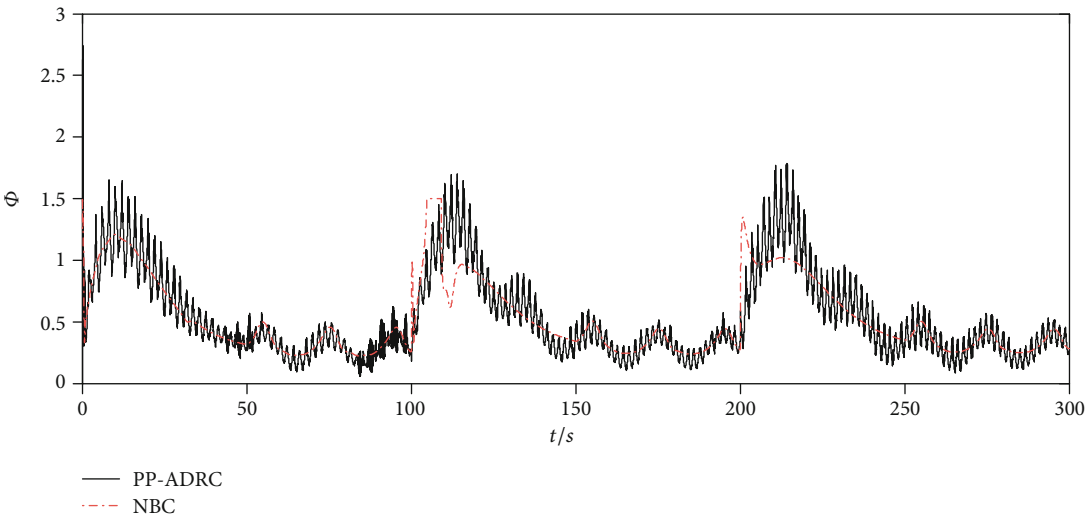

(k) Fuel equivalence ratio

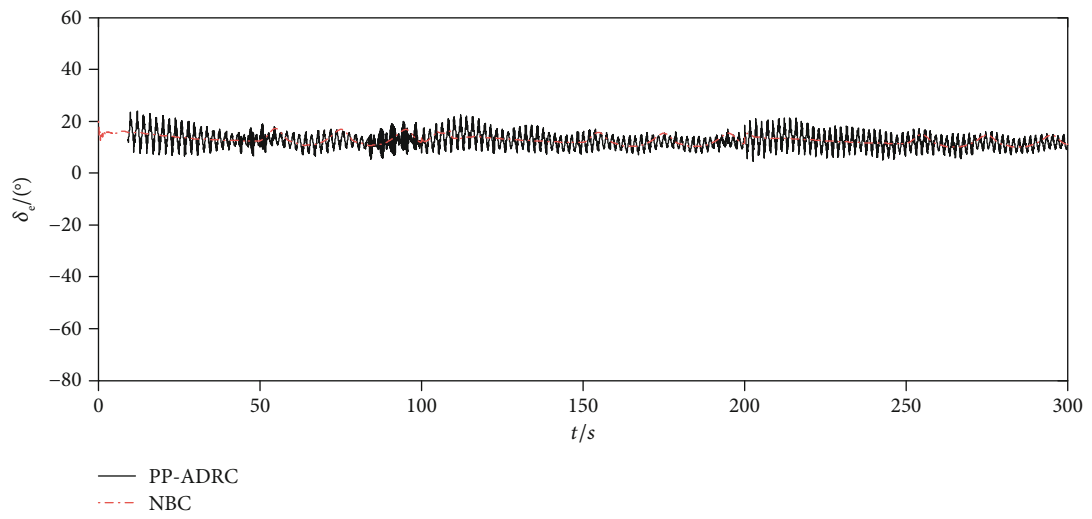

(l) Elevator angular deflection

Figure 4: Simulation results for Scenario 2.

proposed in this paper. The proposed method guarantees the stability of the AHV closed-loop control system. The desired dynamic and steady-state performances of the convergence process of the tracking error were ensured

(2) In the controller design process, the adopted active disturbance rejection method and extended state observer further enhanced the capacity to resist the disturbances, which guaranteed the robustness of the method

(3) The simulation results in the paper proved the effectiveness of the proposed method. The comparison with the related publications showed that the dynamic and steady-state performances of the proposed method were superior

Appendix

A.Proof of Theorem 2

Based on Equations (20)–(22), we set $E^* = Z_2 - H(t) = Z_2 - z_0$. The first derivatives of E and E^* with respect to time can be expressed as follows:

$$\begin{cases} E = Z_1 - z, E^* = Z_2 - z_0, \\ \dot{E} = \dot{Z}_1 - \dot{z} = Z_2 - z_0 - \beta_{01}E = E^* - \beta_{01}E, \\ \dot{E}^* = \dot{Z}_2 - \dot{z}_0 = -G(t) - \beta_{02}|E|^{\alpha_1}\ \mathrm{sgn}\ (E). \end{cases} \tag{A.1}$$

The following Lyapunov function was selected:

$$V = \frac{\beta_{02}}{\alpha_1 + 1} \cdot |E|^{\alpha_1+1} - \sqrt{\frac{2\beta_{02}}{\alpha_1 + 1}} \cdot |E|^{(\alpha_1+1)/2}\ \mathrm{sgn}\ (E) \cdot E^* + \frac{1}{2}E^{*^2}, \tag{A.2}$$

because

$$V = \frac{\beta_{02}}{\alpha_1 + 1} \cdot |E|^{\alpha_1+1} - \sqrt{\frac{2\beta_{02}}{\alpha_1 + 1}} \cdot |E|^{(\alpha_1+1)/2}\ \mathrm{sgn}\ (E) \cdot E^* + \frac{1}{2}E^{*^2} = \left(\sqrt{\frac{\beta_{02}}{\alpha_1 + 1}} \cdot |E|^{(\alpha_1+1)/2}\ \mathrm{sgn}\ (E) - \sqrt{\frac{1}{2}}E^*\right)^2 \geq 0. \tag{A.3}$$

V is positive semidefinite. Below, $\dot{V}$ is studied. The partial derivative of V with respect to E and E^* can be expressed as follows:

$$\frac{\partial V}{\partial E} = \beta_{02}|E|^{\alpha_1}\ \mathrm{sgn}\ (E) - \sqrt{\frac{\beta_{02}(\alpha_1 + 1)}{2}}|E|^{(\alpha_1-1)/2}E^*, \quad \frac{\partial V}{\partial E^*} = -\sqrt{\frac{2\beta_{02}}{\alpha_1 + 1}} \cdot |E|^{(\alpha_1+1)/2}\ \mathrm{sgn}\ (E) + E^*. \tag{A.4}$$

The first derivative of V with respect to time was obtained, and with Equations (70)–(A.1), this yields the following:

$$\begin{aligned} \dot{V} = \frac{\partial V}{\partial E}\dot{E} + \frac{\partial V}{\partial E^*}\dot{E}^* &= \left(\beta_{02}|E|^{\alpha_1}\ \mathrm{sgn}\ (E) - \sqrt{\frac{\beta_{02}(\alpha_1 + 1)}{2}}|E|^{(\alpha_1-1)/2}E^*\right)(E^* - \beta_{01}E) \\ &+ \left(-\sqrt{\frac{2\beta_{02}}{\alpha_1 + 1}} \cdot |E|^{(\alpha_1+1)/2}\ \mathrm{sgn}\ (E) + E^*\right) \\ &\cdot (-G(t) - \beta_{02}|E|^{\alpha_1}\ \mathrm{sgn}\ (E)) \\ &= -\beta_{01}\beta_{02}|E|^{\alpha_1+1} - \sqrt{\frac{\beta_{02}(\alpha_1 + 1)}{2}}|E|^{(\alpha_1-1)/2}E^{*^2} \\ &+ \beta_{01}\sqrt{\frac{\beta_{02}(\alpha_1 + 1)}{2}}|E|^{(\alpha_1-1)/2}E \cdot E^* + \sqrt{\frac{2\beta_{02}}{\alpha_1 + 1}} \\ &\cdot |E|^{(\alpha_1+1)/2}\ \mathrm{sgn}\ (E)G(t) + \beta_{02}\sqrt{\frac{2\beta_{02}}{\alpha_1 + 1}} \cdot |E|^{(\alpha_1+1)/2}|E|^{\alpha_1} \\ &= -\beta_{01}\beta_{02}|E|^{\alpha_1+1} - \sqrt{\frac{\beta_{02}(\alpha_1 + 1)}{2}}|E|^{(\alpha_1-1)/2}E^{*^2} \\ &+ \beta_{01}\sqrt{\frac{\beta_{02}(\alpha_1 + 1)}{2}}|E|^{(\alpha_1+1)/2}\ \mathrm{sgn}\ (E)E^* \\ &+ \sqrt{\frac{2\beta_{02}}{\alpha_1 + 1}} \cdot |E|^{(\alpha_1+1)/2}\ \mathrm{sgn}\ (E)G(t) \\ &+ \beta_{02}\sqrt{\frac{2\beta_{02}}{\alpha_1 + 1}} \cdot |E|^{\alpha_1+1}|E|^{(\alpha_1-1)/2} \\ &\leq -\left(\beta_{01}\beta_{02} - \beta_{02}\sqrt{\frac{2\beta_{02}}{\alpha_1 + 1}}|E|^{(\alpha_1-1)/2}\right)|E|^{\alpha_1+1} \\ &- \left(\sqrt{\frac{\beta_{02}(\alpha_1 + 1)}{2}}|E|^{(\alpha_1-1)/2}\right)E^{*^2} \\ &+ \frac{\beta_{01}}{2}\sqrt{\frac{\beta_{02}(\alpha_1 + 1)}{2}}E^{*^2} + \frac{\beta_{01}}{2}\sqrt{\frac{\beta_{02}(\alpha_1 + 1)}{2}}|E|^{\alpha_1+1} \\ &+ \frac{1}{2}\sqrt{\frac{2\beta_{02}}{\alpha_1 + 1}}|E|^{\alpha_1+1} + \frac{1}{2}\sqrt{\frac{2\beta_{02}}{\alpha_1 + 1}}G^2(t) + \frac{1}{2}E^{*^2} + \frac{1}{2}G^2(t) \\ &= -\left(\beta_{01}\beta_{02} - \beta_{02}\sqrt{\frac{2\beta_{02}}{\alpha_1 + 1}}|E|^{(\alpha_1-1)/2}\right. \\ &\left. - \frac{\beta_{01}}{2}\sqrt{\frac{\beta_{02}(\alpha_1 + 1)}{2}} - \frac{1}{2}\sqrt{\frac{2\beta_{02}}{\alpha_1 + 1}}\right)|E|^{\alpha_1+1} \\ &- \left(\sqrt{\frac{\beta_{02}(\alpha_1 + 1)}{2}}|E|^{(\alpha_1-1)/2} - \frac{\beta_{01}}{2}\sqrt{\frac{\beta_{02}(\alpha_1 + 1)}{2}} - \frac{1}{2}\right)E^{*^2} \\ &+ \left(\frac{1}{2}\sqrt{\frac{2\beta_{02}}{\alpha_1 + 1}} + \frac{1}{2}\right)G^2(t). \end{aligned} \tag{A.5}$$

Values of β_{01}, β_{02}, and α_1 are selected, yielding:

$$\beta_{01}\beta_{02} - \beta_{02}\sqrt{\frac{2\beta_{02}}{\alpha_1+1}}|E|^{(\alpha_1-1)/2} - \frac{\beta_{01}}{2}\sqrt{\frac{\beta_{02}(\alpha_1+1)}{2}} - \frac{1}{2}\sqrt{\frac{2\beta_{02}}{\alpha_1+1}} > 0,$$

$$\sqrt{\frac{\beta_{02}(\alpha_1+1)}{2}}|E|^{(\alpha_1-1)/2} - \frac{\beta_{01}}{2}\sqrt{\frac{\beta_{02}(\alpha_1+1)}{2}} - \frac{1}{2} > 0. \tag{A.6}$$

The following compact set is defined as follows:

$$\Omega_E = \left\{ E \middle| |E| \le \left(\frac{\left((1/2)\sqrt{(2\beta_{02})/(\alpha_1+1)} + (1/2)\right)G^2(t)}{\beta_{01}\beta_{02} - \beta_{02}\sqrt{(2\beta_{02}/\alpha_1+1)}|E|^{(\alpha_1-1)/2} - (\beta_{01}/2)\sqrt{(\beta_{02}(\alpha_1+1)/2)} - 1/2\sqrt{2\beta_{02}/(\alpha_1+1)}} \right)^{1/(\alpha_1+1)} \right\},$$

$$\Omega_{E^*} = \left\{ E^* \middle| |E^*| \le \sqrt{\frac{\left((1/2)\sqrt{(2\beta_{02}/(\alpha_1+1))} + (1/2)\right)G^2(t)}{\sqrt{(\beta_{02}(\alpha_1+1)/2)}|E|^{(\alpha_1-1)/2} - (\beta_{01}/2)\sqrt{(\beta_{02}(\alpha_1+1)/2)} - (1/2)}} \right\}. \tag{A.7}$$

According to Equation (A.4), if $E \notin \Omega_E$ or $E^* \notin \Omega_{E^*}$, then $\dot{V} < 0$. V will decrease until E and E^* converge to the compact sets Ω_E and Ω_{E^*}, respectively. Thus, the error system (Equation (70)) is semiglobally uniformly asymptotically stable. E and E^* are uniformly asymptotically bounded. However, if the radii of the compact sets Ω_E and Ω_{E^*} can be made sufficiently small by selecting appropriate values of β_{01}, β_{02}, and α_1, the errors E and E^* will be sufficiently small, and there must be bounded constants $\sigma_1, \sigma_2 > 0$ such that:

$$\begin{cases} |Z_1 - z| \le \sigma_1, \\ |Z_2 - H(t)| \le \sigma_2. \end{cases} \tag{A.8}$$

Data Availability

The data used to support the findings of this study are available from the corresponding author upon request.

Conflicts of Interest

The authors declare that they have no conflicts of interest.

Acknowledgments

This study was supported by the National Natural Science Foundation of China (Grant no. 61573374 and no. 61703421). The funding did not lead to any conflict of interests.

References

[1] J. J. Bertin and R. M. Cummings, "Fifty years of hypersonics: where we've been, where we're going," *Progress in Aerospace Sciences*, vol. 39, no. 6-7, pp. 511–536, 2003.

[2] E. A. Morelli, "Flight-test experiment design for characterizing stability and control of hypersonic vehicles," *Journal of Guidance, Control, and Dynamics*, vol. 32, no. 3, pp. 949–959, 2009.

[3] D. Preller and M. K. Smart, "Longitudinal control strategy for hypersonic accelerating vehicles," *Journal of Spacecraft and Rockets*, vol. 52, no. 3, pp. 993–999, 2015.

[4] B. Xu and Z. Shi, "An overview on flight dynamics and control approaches for hypersonic vehicles," *Science China Information Sciences*, vol. 58, no. 7, pp. 1–19, 2015.

[5] H. X. Wu and B. Meng, "Review on the control of hypersonic flight vehicles," *Advances in Mechanics*, vol. 39, no. 6, pp. 756–765, 2009.

[6] C. Y. Sun, C. X. Mu, and Y. Yu, "Some control problems for near space hypersonic vehicles," *Acta Automatica Sinica*, vol. 39, no. 11, pp. 1901–1913, 2013.

[7] H. N. Wu, Z. Y. Liu, and L. Guo, "Robust L_∞-Gain fuzzy disturbance observer-based control design with adaptive bounding for a hypersonic vehicle," *IEEE Transactions on Fuzzy Systems*, vol. 22, no. 6, pp. 1401–1412, 2014.

[8] C. Guo, X. G. Liang, J. W. Wang, and H. N. Wu, "Mixed H_2/H_∞ decentralized fuzzy tracking control design for a flexible air-breathing hypersonic vehicle," *Proceedings of the Institution of Mechanical Engineers, Part I: Journal of Systems and Control Engineering*, vol. 229, no. 5, pp. 388–405, 2015.

[9] W. A. Butt, L. Yan, and A. S. Kendrick, "Adaptive dynamic surface control of a hypersonic flight vehicle with improved tracking," *Asian Journal of Control*, vol. 15, no. 2, pp. 594–605, 2013.

[10] X. Wang, J. Guo, S. J. Tang, Q. Xu, Y. Y. Ma, and Y. Zhang, "Robust nonsingular terminal sliding mode backstepping control for air-breathing hypersonic vehicles," *Acta Aeronautica et Astronautica Sinica*, vol. 38, no. 3, pp. 1–13, 2017.

[11] H. Sun, S. Li, and C. Sun, "Finite time integral sliding mode control of hypersonic vehicles," *Nonlinear Dynamics*, vol. 73, no. 1-2, pp. 229–244, 2013.

[12] Y. Wang, C. Jiang, and Q. Wu, "Attitude tracking control for variable structure near space vehicles based on switched nonlinear systems," *Chinese Journal of Aeronautics*, vol. 26, no. 1, pp. 186–193, 2013.

[13] B. Xu, "Robust adaptive neural control of flexible hypersonic flight vehicle with dead-zone input nonlinearity," *Nonlinear Dynamics*, vol. 80, no. 3, pp. 1509–1520, 2015.

[14] B. Xu, Q. Zhang, and Y. Pan, "Neural network based dynamic surface control of hypersonic flight dynamics using small-gain theorem," *Neurocomputing*, vol. 173, pp. 690–699, 2016.

[15] X. Bu, X. Wu, J. Huang, Z. Ma, and R. Zhang, "Minimal-learning-parameter based simplified adaptive neural back-stepping control of flexible air-breathing hypersonic vehicles without virtual controllers," *Neurocomputing*, vol. 175, pp. 816–825, 2016.

[16] X. Bu, X. Wu, R. Zhang, Z. Ma, and J. Huang, "A neural approximation-based novel back-stepping control scheme for air-breathing hypersonic vehicles with uncertain parameters," *Proceedings of the Institution of Mechanical Engineers, Part I: Journal of Systems and Control Engineering*, vol. 230, no. 3, pp. 231–243, 2016.

[17] Z. Gao, Y. Huang, and J. Han, "An alternative paradigm for control system design," in *Proceedings of the 40th IEEE Conference on Decision and Control (Cat. No.01CH37228)*, Orlando, 2001.

[18] Z. Gao, "Active disturbance rejection control: a paradigm shift in feedback control system design," in *2006 American Control Conference*, Minneapolis, 2006.

[19] W. Xue and Y. Huang, "The Active Disturbance Rejection Control for a Class of MIMO Block Lower-Triangular System," in *Proceedings of the 30th Chinese Control Conference*, Yantai, China, 2011.

[20] Y. Huang, W. Xue, G. Zhiqiang, H. Sira-Ramirez, D. Wu, and M. Sun, "Active Disturbance Rejection Control: Methodology, Practice and Analysis," in *Proceedings of the 33rd Chinese Control Conference*, Nanjing, China, July 2014.

[21] B. Z. Guo, Z. H. Wu, and H. C. Zhou, "Active disturbance rejection control approach to output-feedback stabilization of a class of uncertain nonlinear systems subject to stochastic disturbance," *IEEE Transactions on Automatic Control*, vol. 61, no. 6, pp. 1613–1618, 2016.

[22] Z. L. Zhao and B. Z. Guo, "A novel extended state observer for output tracking of MIMO systems with mismatched uncertainty," *IEEE Transactions on Automatic Control*, vol. 63, no. 1, pp. 211–218, 2018.

[23] X. Huang and Q. Ning, "Active disturbance rejection control based on radial basis function neural network," in *2018 IEEE 3rd Advanced Information Technology, Electronic and Automation Control Conference (IAEAC)*, Chongqing, China, October 2018.

[24] B. Zhang, W. Tan, and J. Li, "Tuning of linear active disturbance rejection controller with robustness specification," *ISA Transactions*, vol. 85, pp. 237–246, 2019.

[25] C. Kang, S. Wang, W. Ren, Y. Lu, and B. Wang, "Optimization design and application of active disturbance rejection controller based on intelligent algorithm," *IEEE Access*, vol. 7, pp. 59862–59870, 2019.

[26] Y. Yuan, Z. Wang, Y. Yu, L. Guo, and H. Yang, "Active disturbance rejection control for a pneumatic motion platform subject to actuator saturation: An extended state observer approach," *Automatica*, vol. 107, pp. 353–361, 2019.

[27] C. P. Bechlioulis and G. A. Rovithakis, "Prescribed performance adaptive control of SISO feedback linearizable systems with disturbances," in *2008 16th Mediterranean Conference on Control and Automation*, Ajaccio, France, June 2008.

[28] H. Y. Li, J. N. Xu, J. P. Zhang, G. P. Zhang, and K. P. Zheng, "Backstepping control with prescribed performance for longitudinal inner-loop system of hypersonic vehicles," *Aero Weaponry*, vol. 4, no. 2, pp. 24–28, 2016.

[29] P. F. Wang, J. Wang, J. M. Shi, and C. Luo, "Prescribed performance back-stepping robustness control of a flexible hypersonic vehicle," *Electric Machines and Control*, vol. 21, no. 2, pp. 94–102, 2017.

[30] X. B. Li, S. Y. Zhao, X. W. Bu, and Y. G. He, "Design of prescribed performance backstepping control for hypersonic vehicles," *Journal of Beijing University of Aeronautics and Astronautics*, vol. 45, no. 4, pp. 650–661, 2019.

[31] X. Bu, X. Wu, J. Huang, and D. Wei, "A guaranteed transient performance-based adaptive neural control scheme with low-complexity computation for flexible air-breathing hypersonic vehicles," *Nonlinear Dynamics*, vol. 84, no. 4, pp. 2175–2194, 2016.

[32] J. Q. Han, "Auto disturbances rejection control technique," *Frontier Science*, vol. 1, no. 1, pp. 24–31, 2007.

[33] M. A. Bolender and D. B. Doman, "A non-linear model for the longitudinal dynamics of a hypersonic air-breathing vehicle," in *AIAA Guidance, Navigation, and Control Conference and Exhibit*, pp. 1–22, San Francisco, California, August 2005.

[34] M. A. Bolender and D. B. Doman, "Nonlinear longitudinal dynamical model of an air-breathing hypersonic vehicle," *Journal of Spacecraft and Rockets*, vol. 44, no. 2, pp. 374–387, 2007.

[35] J. T. Parker, A. Serrani, S. Yurkovich, M. A. Bolender, and D. B. Doman, "Control-oriented modeling of an air-breathing hypersonic vehicle," *Journal of Guidance, Control, and Dynamics*, vol. 30, no. 3, pp. 856–869, 2007.

[36] C. P. Bechlioulis and G. A. Rovithakis, "Robust adaptive control of feedback linearizable MIMO nonlinear systems with prescribed performance," *IEEE Transactions on Automatic Control*, vol. 53, no. 9, pp. 2090–2099, 2008.

[37] X. Bu, "Guaranteeing prescribed output tracking performance for air-breathing hypersonic vehicles via non-affine back-stepping control design," *Nonlinear Dynamics*, vol. 91, no. 1, pp. 525–538, 2018.

[38] X. Bu, "Guaranteeing prescribed performance for air-breathing hypersonic vehicles via an adaptive non-affine tracking controller," *Acta Astronautica*, vol. 151, pp. 368–379, 2018.

[39] L. Fiorentini and A. Serrani, "Adaptive restricted trajectory tracking for a non-minimum phase hypersonic vehicle model," *Automatica*, vol. 48, no. 7, pp. 1248–1261, 2012.

[40] L. Fiorentini, A. Serrani, M. A. Bolender, and D. B. Doman, "Nonlinear robust adaptive control of flexible air-breathing hypersonic vehicles," *Journal of Guidance, Control, and Dynamics*, vol. 32, no. 2, pp. 402–417, 2009.

[41] B. Z. Guo and Z. L. Zhao, "Weak convergence of nonlinear high-gain tracking differentiator," *IEEE Transactions on Automatic Control*, vol. 58, no. 4, pp. 1074–1080, 2013.

[42] Q. Guoyuan, C. Zengqiang, and Y. Zhuzhi, "New tracking-differentiator design and analysis of its stability and convergence," *Journal of Systems Engineering and Electronics*, vol. 15, no. 4, pp. 780–787, 2004.

[43] B. Xu, D. X. Gao, and S. X. Wang, "Adaptive neural control based on HGO for hypersonic flight vehicles," *Science China Information Sciences*, vol. 54, no. 3, pp. 511–520, 2011.

[44] X. Bu, X. Wu, R. Zhang, Z. Ma, and J. Huang, "Tracking differentiator design for the robust backstepping control of a flexible air-breathing hypersonic vehicle," *Journal of the Franklin Institute*, vol. 352, no. 4, pp. 1739–1765, 2015.

[45] X. Bu, X. Wu, Z. Ma, R. Zhang, and J. Huang, "Novel auxiliary error compensation design for the adaptive neural control of a constrained flexible air-breathing hypersonic vehicle," *Neurocomputing*, vol. 171, pp. 313–324, 2016.